

# **PEER TO PEER ENERGY TRADING PLATFORM: HARDWARE AND SOFTWARE INTEGRATION**

A DISSERTATION SUBMITTED IN PARTIAL FULFILLMENT  
OF THE REQUIREMENTS FOR THE DEGREE OF

**MASTER OF TECHNOLOGY**

IN  
DISCIPLINE OF ELECTRICAL ENGINEERING,

BY

ANANDSINGH P. CHAUHAN

ROLL NO: 18250004



**INDIAN INSTITUTE OF TECHNOLOGY GANDHINAGAR**

**GUJARAT, INDIA**

**JULY, 2020**

## **CERTIFICATE**

It is certified that the work contained in the thesis titled **Peer to Peer Energy Trading Platform: Hardware and Software Integration** by **Anandsingh P. Chauhan (18250004)**, has been carried out under my supervision and that this work has not been submitted elsewhere for a degree.

**Dr. Naran M. Pindoriya**  
Associate Professor, Electrical Engineering  
Indian Institute of Technology Gandhinagar  
Palaj, Gandhinagar-382355, Gujarat

© ANANDSINGH P. CHAUHAN

---

2023

**D E D I C A T I O N**

---

To the Almighty God and my family

---

## A C K N O W L E D G M E N T S

---

I am deeply grateful to my thesis supervisor Dr. Naran Pindoriya, for providing me the opportunity to work on this wonderful project. He made sure of his continuous availability for discussion and guidance inspite of his busy schedule. I would like to thank Department of Science and Technology, and Institute for providing the necessary infrastructure. I thank my project team: Dr. Joice Phillip, Ravindra Kuhada, Dr. Shivashankar, and Sachin Suthar for the valuable discussions, and suggestions in the duration of my work in the project. I would thank to advisory committee members, Prof. S. Rajendran and Prof. Atul Bhargav. I would also thank all members of the PS&SG lab for providing a great company during my tenure at IIT Gandhinagar. I would like to express my gratitude and thank my parents for supporting me throughout life.

---

## Table of Contents

<b>Dedication</b> . . . . .	<b>i</b>
<b>Acknowledgments</b> . . . . .	<b>ii</b>
<b>List of Figures</b> . . . . .	<b>v</b>
<b>List of Tables</b> . . . . .	<b>vii</b>
<b>List of Abbreviations</b> . . . . .	<b>viii</b>
<b>Abstract</b> . . . . .	<b>ix</b>
<b>Chapter</b>	
<b>1 Introduction</b> . . . . .	<b>1</b>
1.1 Background . . . . .	1
1.2 Literature Survey . . . . .	2
1.3 Thesis Objective . . . . .	3
1.4 Thesis Organization . . . . .	5
<b>2 P2P Energy Trading</b> . . . . .	<b>6</b>
2.1 Introduction . . . . .	6
2.2 Peer Description . . . . .	6
2.2.1 Peer A . . . . .	6
2.2.2 Peer B . . . . .	9
2.2.3 Peer C . . . . .	11
2.3 Forecasting . . . . .	11
2.4 Integration of Energy Meter and Smart Agent . . . . .	12
2.5 Database in Smart Agent . . . . .	16
2.6 Integration of Hardware and Software Layer . . . . .	18
2.6.1 P2P Trading Steps . . . . .	18
2.6.2 Node Application and Smart Agent . . . . .	19
2.7 Results and Discussions . . . . .	21
2.7.1 Base Case . . . . .	21
2.7.2 Deterministic Case . . . . .	25
2.7.3 P2P Energy Trading . . . . .	27
2.8 Summary . . . . .	29
<b>3 Grid Connected Bidirectional Converter</b> . . . . .	<b>30</b>
3.1 Introduction and Literature Survey . . . . .	30
3.2 Vehicle to Grid (V2G) . . . . .	31
3.3 Battery Discharging Characteristics . . . . .	32

3.4 Methodology : Battery Power Flow Control . . . . .	33
3.4.1 Hysteresis Band Control . . . . .	37
3.5 Results . . . . .	38
3.6 Summary . . . . .	40
<b>4 Conclusion and Future Work . . . . .</b>	<b>41</b>
4.1 Conclusion . . . . .	41
4.2 Scope for Future Work . . . . .	42
<b>References . . . . .</b>	<b>44</b>

## List of Figures

1.1	Layout of testbed at WTP, IIT Gandhinagar . . . . .	4
1.2	Different layers of testbed . . . . .	4
2.1	Schematic diagram of Peer A . . . . .	7
2.2	Schematic diagram of Peer B . . . . .	9
2.3	Schematic diagram of Peer C . . . . .	11
2.4	PV forecast . . . . .	12
2.5	RS 485 and energy meter integration . . . . .	13
2.6	Flow diagram for communication with energy meter . . . . .	13
2.7	Database in smart agent . . . . .	16
2.8	All meter table in database . . . . .	17
2.9	Historical data table in database . . . . .	17
2.10	Forecasting table in database . . . . .	18
2.11	Optimization table in database . . . . .	18
2.12	Schematic representation of hardware and software layer integration . . . . .	19
2.13	Smart agent data in the JSON format in cloud using AP . . . . .	21
2.14	P2P trading setup at WSC -II . . . . .	22
2.15	PV and load profile of Peer A . . . . .	22
2.16	Electricity price . . . . .	23
2.17	Peer B load profile . . . . .	23
2.18	BESS power dispatch & SOE (case 1) . . . . .	24
2.19	Grid power dispatch (case 1) . . . . .	24
2.20	BESS power dispatch & SOE (case 2 DA tariff) . . . . .	25
2.21	Grid power dispatch (case 2 DA tariff) . . . . .	25
2.22	BESS power dispatch & SOE (case 2 ToU tariff) . . . . .	26
2.23	Grid power dispatch (case 2 ToU tariff) . . . . .	26
2.24	Trade creation in the android application . . . . .	28
2.25	Battery status during energy trading . . . . .	28
2.26	Blockchain smart contract with transaction details . . . . .	29



3.1	Block diagram of the V2G mode of operation of an EV . . . . .	32
3.2	Battery discharging behaviour to different C rates . . . . .	33
3.3	Grid integration of EV battery . . . . .	34
3.4	Control strategy of DC-DC bidirectional converter . . . . .	34
3.5	Park transformation . . . . .	35
3.6	Control strategy of grid connected bidirectional converter . . . . .	36
3.7	Hysteresis current controller . . . . .	37
3.8	Active power dispatch to grid . . . . .	38
3.9	SOC, battery current & battery voltage . . . . .	39
3.10	AC current (RMS) . . . . .	39
3.11	PCC voltage and current . . . . .	40

## List of Tables

1.1	Load Details of Peers at Testbed . . . . .	4
2.1	Nomenclature . . . . .	7
2.2	Peer A Battery Parameters . . . . .	7
2.3	EV Battery Parameters of Peer B . . . . .	10
2.4	Modbus Settings . . . . .	15
2.5	APIs for Communication with Digital Platform . . . . .	20
2.6	Comparison Between Base Case and Deterministic Case . . . . .	27
3.1	Battery Current References . . . . .	38

## **List of Abbreviations**

<b>BESS</b>	Battery Energy Storage System
<b>DA</b>	Day Ahead
<b>EV</b>	Electric Vehicle
<b>G2V</b>	Grid to Vehicle
<b>HCC</b>	Hysteresis Current Control
<b>IEX</b>	Indian Energy Exchange
<b>ToU</b>	Time of Use
<b>P2P</b>	Peer to Peer
<b>PLL</b>	Phase Locked Loop
<b>PCC</b>	Point of Common Coupling
<b>SRF</b>	Synchronous Reference Frame
<b>UPF</b>	Unity Power Factor
<b>V2G</b>	Vehicle to Grid
<b>WSC</b>	Water Service Centre
<b>WTP</b>	Water Treatment Plant

## **Abstract**

The energy sector is undergoing a massive transformation that includes key aspects such as integrating renewables, improving operational efficiency, leveraging smart grid infrastructure, and handling the dynamics of transactive energy. Digitization of electricity value chain and increased integration of distributed energy resources are turning passive consumers into active consumers who can locally sell their electricity, called Prosumers. The Peer to Peer (P2P) energy trading is a new paradigm, which introduces flexibility among the electricity users, where the energy from renewables and battery storage is shared and traded locally.

This thesis contributes to the realisation of the hardware and software platform for P2P energy trading testbed at IIT Gandhinagar. This setup comprises two prosumers (Peer A and Peer B) and a consumer (Peer C). Peer A has solar PV, and battery energy storage system, whereas Peer B has an EV charging with a vehicle to grid (V2G) capability. These peers have almost equal load demand to meet. The energy meters connected at the respective nodes are integrated with a smart agent to log the energy data at the regular interval. A smart agent runs the forecasting module followed by an optimization algorithm to optimally schedule the dispatchable resources at the respective peers. This setup has been seamlessly interfaced with Blockchain based digital platform for showcasing the P2P energy trading application in a real world environment.

# Chapter 1

## Introduction

### 1.1 Background

Energy sector is undergoing a massive transformation that includes key aspects such as integrating renewables, improving operational efficiency, leveraging smart grid infrastructure, and handling the dynamics of Transactive energy. Indian market of solar PV saw a 72% growth in financial year 2019 over financial year 2018 with installed rooftop capacity of 4,375 MW, and shares around 14% of the cumulative solar in India. The Paris declaration on electric vehicles (EVs) and climate change is a crucial element to the shift from bio-fuel-based vehicles to EVs, which aims for the international deployment of 100 million EVs by 2030 [1]. By using a bidirectional charger, consumers can discharge its EV battery, keeping in consideration price, and SOC. However, as the penetration of these distributed energy sources increases, the entities/consumers will have surplus energy, which will eventually be injected into the main grid. This method is known as the feed-in tariff (FiT) scheme, and such entities are known as prosumers, also called proactive consumers [2].

Prosumers have a vital role to play in deregulated energy markets. The main disadvantage of the DER is that the energy obtained from these sources are intermittent in nature. However, a high degree of DER penetration adversely affects the stability of the main grid, due to which energy export limits will be enforced on the prosumers. Further, the economic benefits of supplying surplus energy to the main grid are not significant. Due to the above reasons, the FiT scheme is not very prevalent in energy markets [2].

Peer to Peer (P2P) energy trading [3], [4] is an alternative of the current FiT scheme, which can be regarded as the energy management system for the smart grid, where the prosumer trades the surplus energy with another prosumer or a consumer without the influence of a central controller.

The main limitation of the P2P energy trading is the absence of central controller, which reduces its trustworthiness, but blockchain's distributed ledger technology for recording the transactions eliminates the risks and maintains trust and transparency. P2P markets are designed with a consumer-centric approach and consumers to have the

option of choosing the source of their energy [5]. Piclo, Vandebrom, Peer Energy cloud, Brooklyn microgrid, and SonnenCommunity are some of the ongoing P2P energy trading projects [6].

## 1.2 Literature Survey

The first P2P concept was introduced in 2007 [7], and the first working project using P2P sharing energy in the local area is the Brooklyn microgrid [6]. In this, excess solar PV power has been sold to other peer in the same microgrid using Ethereum blockchain. A hierarchical system architecture for P2P energy trading is proposed in [8], wherein the peers can shift their role between a prosumer and consumer. An optimization model for maximizing the economic benefits of P2P energy trading of different entities having solar PV system with and without energy storage is introduced in [9]. Two-stage control method for P2P energy trading in community networks where the requirement of communication equipment is greatly reduced is proposed in [10]. P2P energy trading using blockchain-based coalition algorithms between microgrids is proposed in [11]. This algorithm is found to converge faster and better scalable than existing coalition algorithms. P2P energy trading using game-theoretic models is proposed in [12]. In this work, stackelberg game theory is used to model pricing competition between sellers and buyers, while competition between sellers is modeled as a cooperative peers.

P2P energy trading model is proposed in [13], which helps to reduce prosumers demand through a Stackelberg cooperative game during the day's peak hours. Here, the central power system acts as the leader, and prosumers act as followers. The central power system determines the cost of energy at the peak periods, and the prosumers who curtail their demand during the peak period are given monetary incentives. A distributed P2P day ahead trading method for multi-microgrids using game theory is proposed in [14]. A non-cooperative game and stackelberg game model were developed to analyze the relationship between sellers and buyers. The effect of adding network constraints in P2P energy trading through sensitivity analysis is studied in [11], [15]. The effectiveness of using energy storage systems in P2P trading is investigated in [16] through flexible market and designs. A P2P energy trading model based on multi bilateral trading and product differentiation is proposed in [17]. The main advantage of model presented in [17] is that it can be implemented without the requirement of a central agent using a distributed relaxed consensus and innovation approach. The role of middlemen or energy brokers in customer to customer energy trading in an event-driven market using reinforcement learning is explored in [18]. This model helps to improve market efficiency and attain better localized power balance while considering the characteristics of customers behavior also into account.

P2P energy trading with EVs is proposed in [19], it reduces the effect of EV charging

during peak hours on the electrical grid. The study of the vehicle to the grid using the bidirectional converter is carried out in most of the literature. The study of the allowable harmonics limit into the grid has been carried out in IEEE 1547 [20], SAE-J2894 [21], IEC1000-3-2 [22]. The battery charger topologies, charging types, and levels are discussed into [23]. The different system design of an EV charging station been carried out in [1]. The numerous EV-PV topologies and EV-PV converters were also addressed for achieving vehicle to grid (V2G). Two optimization models for individual optimal charging algorithms and P2P energy trading between EVs are proposed in this work. P2P energy trading between PhEVs is proposed in [24]. An iterative double auction mechanism is used for identifying the buying and selling price of electricity. Further, a blockchain technology is also used in this model to improve transaction security.

### 1.3 Thesis Objective

This thesis a part of the DST - Mission Innovation project titled “Prosumer driven integrated smart grid” [25], which aims to develop a blockchain based platform for peer to peer energy trading. The project headed by IIM Ahmedabad has both industrial partners (BSES, Renault Nissan, Amplus Solar) and academic partners (IIT Gandhinagar). The design, development, and lab testing of the P2P energy trading test-bed is carried out by IIT Gandhinagar. Fig. 1.1 shows the layout of the three peers test-bed setup. The setup is developed at the Water Service Center (WSC - II) at IIT Gandhinagar. Such test-bed and lab testing aim to debug and to troubleshoot the system-level design.

From the literature review, it can be inferred that P2P energy trading is a well researched topic. However, experimental validation of the proposed algorithm is not done in most of these works [9],[26],[19]. In the proposed model, peers involved managing their electrical energy requirement among themselves such that the power drawn from the main grid as well as the electricity bill is minimized. It also helps the peers to efficiently utilising their energy resources, while maintaining the data and energy security and increasing renewable energy share.

Among these peers, Peer A and Peer B are prosumers as they have a solar PV with battery and an EV, respectively. The third peer, i.e., Peer C, does not have any energy storage; hence it is purely a consumer. The Table 1.1 describes peer informations. The proposed model helps in effective energy trade between these three peers, such that the economic benefits of these peers are improved compared to that of the FiT scheme.

The proposed P2P testbed has three layers, namely hardware layer, control layer and smart agent layer. The hardware layer comprises of solar PV, EV, load, battery and meters associated with these devices. The energy meter readings with the associated meters go inside the smart agent database. This database is made inside the MySQL of the smart agent and uses a phpmyadmin web application based GUI for managing

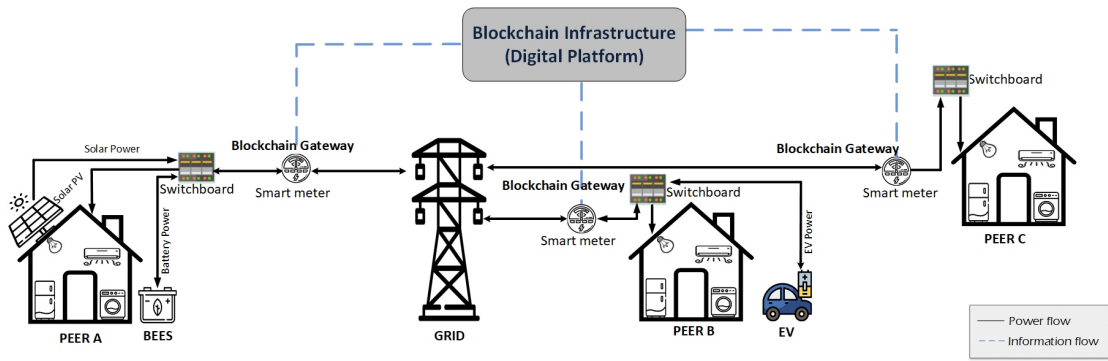


Figure 1.1: Layout of testbed at WTP, IIT Gandhinagar

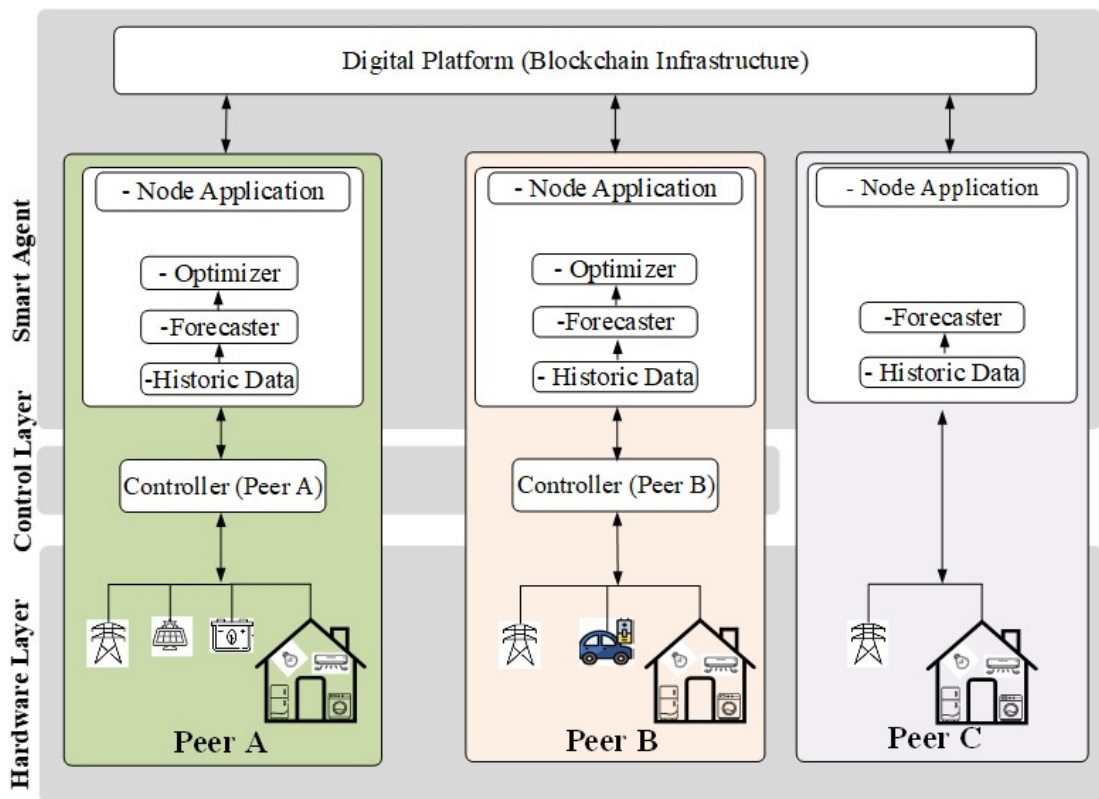


Figure 1.2: Different layers of testbed

Table 1.1: Load Details of Peers at Testbed

	Battery (kWh)	Load (kW)	PV (kW)
Peer A	7.5	2	3
Peer B	3.75	3	-
Peer C	-	3.5	-

the database. All energy meters are identified by a unique IDs. The data from the meters are sampled and inserted into the historical table of the smart agent database.



The solar forecasting and load forecasting model uses the stored data in historical table for accurately predicting the day ahead solar PV generation and load output, which are later saved into the forecast table of the database. The forecasting table data later used by the optimizer for the scheduling of the battery charging and discharging profile for every fifteen minutes.

The next step is to schedule the battery as per the optimization result, and the control layer plays an important role. It receives a signal from the microcontroller and manages power flow as per schedules given by energy management formulation. The control layer contains the controllers to schedule the battery as per the optimization result. It requires a signal from the microcontroller.

In the third layer a node application is running inside the smart agent. It is a node.js file and used for a real-time application, which is to fetch data from the table and to show the user.

## **1.4 Thesis Organization**

The brief introduction about the testbed peers, linear regression method for solar PV and load forecasting, and the formulation of an energy management algorithm for optimal scheduling of a BESS and an EV are presented in chapter 2. The communication protocols, smart agent, its database are also discussed in this chapter. A comparison between the base case and the deterministic case also discussed. The test of trade between two peers and the transaction details of the trade also addressed at the end of the chapter.

In chapter 3, A control strategy of power electronic converters is discussed to achieve vehicle to grid feature of an EV, besides G2V. The schedules for V2G are obtained from the EV smart charging algorithm presented in chapter 2. The chapter concludes with the simulation results.

Chapter 4 concludes the thesis with some suggestions for future work.

## Chapter 2

# P2P Energy Trading

### 2.1 Introduction

Peer to Peer (P2P) energy trading platform at IIT Gandhinagar is as shown in Fig. 1.1. The testbed comprises two prosumers (Peer A and Peer B) and a consumer (Peer C). Peer A has solar PV, and battery energy storage system, whereas Peer B, has an EV charging with a vehicle to grid (V2G) capability. These peers have almost equal load demand to meet. The trade has been conducted between two Peers of the trading platform, and the result of P2P energy trade is included in the chapter. A minimal modbus module is used for extracting the energy meter readings and stored as historical data. The linear regression-based method is used for the forecasting of solar PV power and load. A linear programming based formulation is used for Peers to manage their energy consumption effectively. Energy management formulations aim to increase locally generation and cost minimization of electricity. The optimization algorithm formulated considering battery charging and discharging power, SOE constraints, grid constraints. The real-time data collected in the database of the smart agent is used as the input parameters of the presented algorithm. A base case scenario and the deterministic scenario of the energy management formulation of Peer A has also been compared at the end of the chapter.

### 2.2 Peer Description

#### 2.2.1 Peer A

The schematic diagram of Peer A is given below in Fig. 2.1. As evident from the Fig. 2.1, it has a solar PV of 3 kW and a BESS of 7.5 kWh. Solar PV generates energy during the day, which is used for fulfilling the residential energy requirement and for charging the battery. The surplus energy, if present, will be used for P2P energy trading. Energy meters are connected at different locations of Peer A to measure the residential consumption, solar PV generation, battery charging or discharging, and the net power

Table 2.1: Nomenclature

$C$	Electricity price
$C_{rate}$	Charge and discharge rate of EV battery
$P^{bc}$	Battery charging power
$P^{bd}$	Battery discharging power
$P^l$	Forecasted load demand
$P^g$	Utility grid power
$P^{pv}$	Forecasted solar PV generation
$SOE$	State of energy
$SOE_0$	Initial state of energy
$T$	Total time intervals
$\eta^{bc}$	Battery charging efficiency
$\eta^{bd}$	Battery discharging efficiency

consumption. These meters continuously measure the power and energy consumed at 15-minute intervals, which are later saved into the historical table created in the smart agent database. The smart agent communicates with the meters through serial communication using the Modbus RTU protocol, and the communication standard used is RS 485.

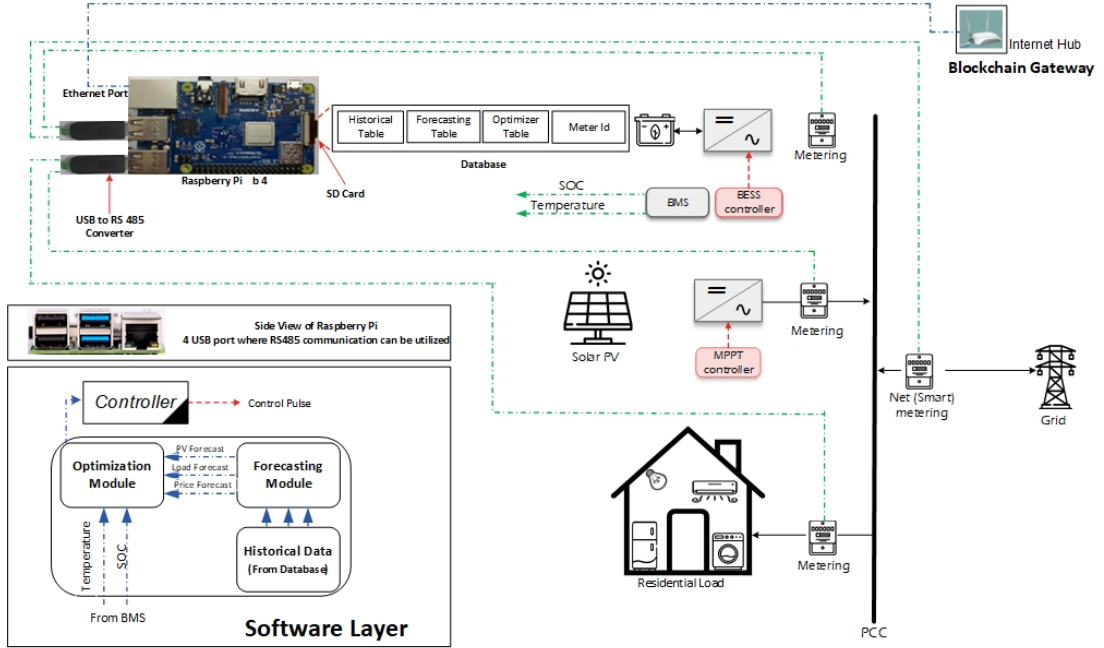


Figure 2.1: Schematic diagram of Peer A

Table 2.2: Peer A Battery Parameters

$E^b$	$SOE_0$	$SOE_{min}$	$SOE_{max}$	$P_{min}^{bc}, P_{min}^{bd}$	$P_{max}^{bc}, P_{max}^{bd}$	$\eta^c, \eta^d$
7.5 kWh	3.5 kWh	1.5 kWh	6.75 kWh	0 kW	3.3 kW	97%

$$Cost = \sum_{t=1}^T (C_t^f P_t^g \Delta t) \quad (2.1)$$

$$P_t^g + P_t^{PV} + P_t^{bd} = P_t^{bc} + P_{t,s}^g \quad (2.2)$$

$$SOE_t^b = SOE_{t-1}^b + [(P_t^{bc} \eta^{bc} - \frac{P_t^{bd}}{\eta^{bd}}) \Delta t] \quad (2.3)$$

$$SOE_T^b = SOE_0^b \quad (2.4)$$

$$P_t^{PV} + P_t^{bd} \leq P_{max}^{Inv} \quad (2.5)$$

$$P_{min}^{bc} \leq P_t^{bc} \leq P_{max}^{bc} \quad (2.6)$$

$$P_{min}^{bd} \leq P_t^{bd} \leq P_{max}^{bd} \quad (2.7)$$

$$P_{min}^g \leq P_t^g \leq P_{max}^g \quad (2.8)$$

$$SOE_{min} \leq SOE_t \leq SOE_{max} \quad (2.9)$$

The objective of Peer A is the cost minimization of its electricity bill and maximize the P2P energy traded, thereby reducing the power drawn from the main grid. The formulated equations can be mathematically represented as (2.1)

Here, (2.2) refers to the power balance equation. It states that the sum of grid power, solar PV power, and battery discharge power will always be equal to the amount of load consumption and battery charging power. As the proposed P2P energy trading model works like a day-ahead market, the solar power generation and load consumption of the next day is required for this power balance equation. Although the solar PV generation and the load consumption will be changing continuously, a near accurate estimate of these quantities can be forecasted using regression techniques. In this model, a linear regression method is used for forecasting these values. The forecasted values of the load consumption and solar PV generation are stored in the all\_forecast table in the smart agent.

The state of energy (SOE) of the battery is mathematically expressed in (2.3) and (2.4). The SOE of the battery at a particular instant is the sum of SOE at the previous instant and the battery charging or discharging energy. This is mathematically represented in (2.3). It should be noted that the battery can either be charged or discharged at a time. The SOE of the battery will be the same at the starting and ending periods. This is mathematically expressed in (2.4). (2.5) to (2.8) represent the limits of the grid power, battery charging and discharging power and SOE.

The optimal scheduling of the battery is obtained after the objective function in (2.1) is minimized subject to the constraints listed in (2.2) to (2.8). The results of linear programming are stored in the all\_optimizer table created in the smart agent.

## 2.2.2 Peer B

Schematic diagram of Peer B is shown in Fig.2.2. Peer B has an EV having a battery of 4.096 kWh. The fully charged EV battery can be used either for its trips or for self-consumption. It can also be used for supplying power to other consumers during periods of high demand thereby helping in peak shaving. Peer B load is the drainage pump, dosing pump, ICB lights and the compressor pump of WSC II. Smart meters are connected at different locations of Peer B to measure the residential consumption, EV battery charging or discharging and the net power consumption. These meters continuously measure the power and energy consumed at 15-minute intervals which are later saved into the historical table created in the smart agent.

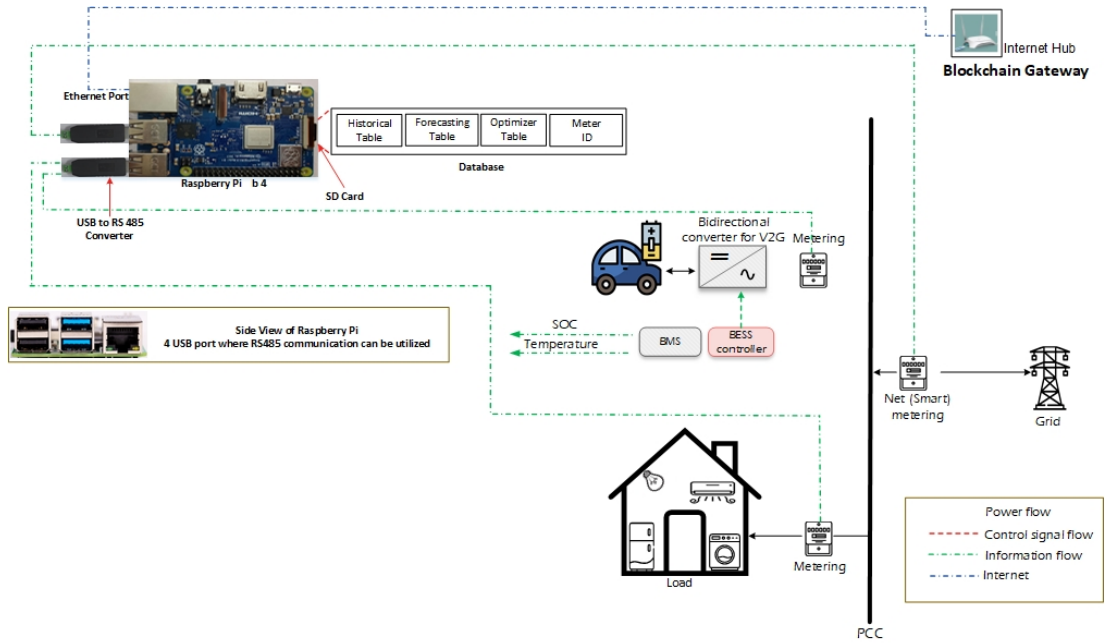


Figure 2.2: Schematic diagram of Peer B

Peer B aim is the cost minimization of its electricity bill by optimally scheduling the electric vehicle (EV) battery charging and discharging schedules considering the electricity price. This is mathematically represented as the schematic representation of Peer B. As evident from the Fig. 2.2, it has an EV with a battery of 4.096 kWh, 48V. The battery charges during off-peak hours, which is later used for its trips. Further, depending on the DoD of battery or the SOE of the battery, it is used to supply power at peak hours, thereby reducing the electricity bill.

$$Cost = \sum_{t=1}^T (C_t^f P_t^g \Delta t) \quad (2.10)$$

Table 2.3: EV Battery Parameters of Peer B

$E_b$	$V_{oc}$	$Q_b$	$I_{bc}$	$I_{bd}$
4.096 kWh	51.2 V	75 Ah	40 A	75 A

$$P_t^g + P_t^{bd} = P_t^{bc} + P_t^l \quad (2.11)$$

$$SOE_t^b = SOE_{t-1}^b + [(P_t^{bc}\eta^{bc} - \frac{P_t^{bd}}{\eta^{bd}})\Delta t] \quad (2.12)$$

$$SOE_T^b = SOE_0^b \quad (2.13)$$

$$SOE_{T_d}^b = SOE_{max}^b \quad (2.14)$$

$$T_a \leq t \leq T_d \quad (2.15)$$

$$P_{min}^{bc} \leq P_t^{bc} \leq P_{max}^{bc} \quad (2.16)$$

$$P_{min}^{bc} \leq P_t^{bd} \leq P_{max}^{bd} \quad (2.17)$$

$$I_t^{bd} \leq 1C_{rate} \quad (2.18)$$

$$P_{min}^g \leq P_t^g \leq P_{max}^g \quad (2.19)$$

$$SOE_{min}^b \leq SOE_t^b \leq SOE_{max}^b \quad (2.20)$$

Here  $P_t^g$ ,  $P_t^{bc}$ ,  $P_t^{bd}$ ,  $SOE_t$  represents the grid power, battery charging power, battery discharging power and state of energy at instant t of Peer A.  $T_a$  and  $T_d$  denote the arrival and departure times of EV. The EV can be used as energy storage only during the time period  $t = \{T_a, T_d\}$ .

(2.11) represents the power balance equation. It shows that the sum of the power drawn from the grid and battery discharge power is equal to the sum of load consumption and battery charging power. As the proposed P2P energy trading model works like a DA market, the next day's load consumption is required for this power balance equation. Hence, the load is forecasted using the linear regression model explained in section 2.7. Further, the forecasted values are saved into the all\_forecast table in the smart agent database.

(2.12), (2.14) shows the SOE of the battery at various time intervals. It is observed from (2.12) that the SOE of the EV at a particular instant is the sum of its SOE at the previous instant and battery charging or discharging energy. This equation is valid only in the time interval  $\{T_a, T_d\}$  as the EV will be available at home for energy storage. The SOE of the battery is maximum at  $t = \{T_d\}$ . This is expressed in (2.14). The lower and upper limits of grid power, battery charging and discharging power and SOE are given in (2.18) to (2.20).

The optimal EV battery scheduling is obtained by minimizing the objective function subjected to the constraints shown in Eqns. (2.10) to (2.20). The result obtained from

this optimization is stored in the all\_optimization table of the database.

### 2.2.3 Peer C

Fig. 2.5 shows the schematic representation of Peer C. It is observed that, unlike Peer A and Peer B, Peer C does not have any energy storage device or solar PV connected to it. Hence, this peer acts only as a consumer.

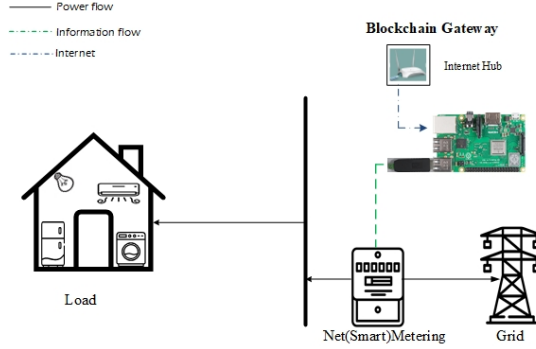


Figure 2.3: Schematic diagram of Peer C

A smart meter is connected at the point of common coupling to measure the load consumption of Peer C at 15-minute intervals. The measured value is fed into the historical table in the smart agent database.

## 2.3 Forecasting

The output of the solar PV varies from time to time, as explained in chapter 1. This intermittent operation leads to a high degree of uncertainty and harms the power grid, of late; battery energy storage systems are used along with solar PV to reduce this uncertainty. The economic operation of the P2P energy trading model requires balancing of the generation and demand. Therefore, forecasting of the renewable energy generation and load is essential for making the model profitable. In the proposed model, a linear regression-based forecasting model is used to forecast the load and renewable energy generation.

In the proposed model, the load and solar PV output are forecasted using the historical data of the previous 30 days. These are obtained from the smart meters placed at different peers at an interval of 15 minutes. Out of these 30, 23 days data are used to train the model, and the remaining seven days data are used to test the model. The predicted output and actual output are compared by using the MSE and variance score.

$$MSE = \frac{1}{n} \sum_{i=1}^n (y_i - \hat{y}_i)^2 \quad (2.21)$$

$$Variance = \frac{\sum_{i=1}^n (y_i - \hat{y}_i)^2}{n - 1} \quad (2.22)$$

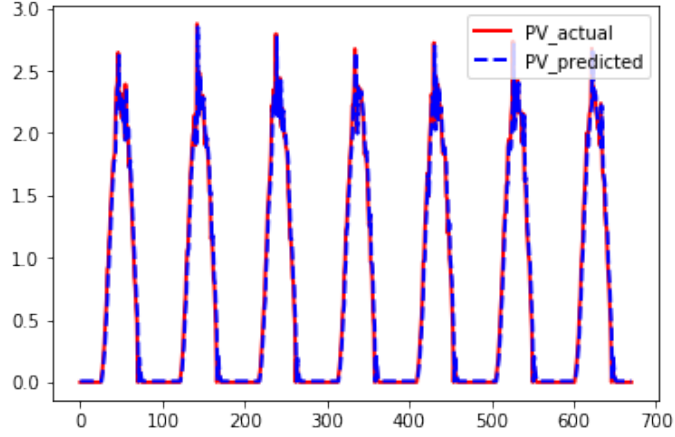


Figure 2.4: Solar PV forecast

Fig. 2.4 shows the forecasted and actual output of the solar PV at Peer A. It is observed that the curve of the forecasted data is almost similar to that of the actual data. Further, the mean squared error and the variance of the proposed model are found to be 0.71 and 0.92 respectively. This proves that the proposed linear regression-based model provides accurate forecasts of PV.

The results of the forecasting algorithm are as follows:

- Mean squared error: 0.71
- Variance score: 0.92

## 2.4 Integration of Energy Meter and Smart Agent

The data measured using the energy using the energy meters is fetched using RS 485, and it is stored in the smart agent database. RS 485 is a serial transmission standard and it is advantageous in terms of the number of devices connected at one particular node.

Any number of instruments can be connected to the RS 485 bus. It is generally consisting of two wires, which are carrying differential voltages. A resistor of  $120 \Omega$  is connected at the termination end. Typically, both lines are at the same voltage but whenever transmission occurs, one of the lines is pulled towards higher potential. Every transceiver chip has both transmitter and receiver.

A modbus wire is configured to all the energy meters in the communication layer. Each meter will have a unique ID, which is used by the smart agent for identifying the data measured by them. A general-purpose microcontroller is used as smart agent here,



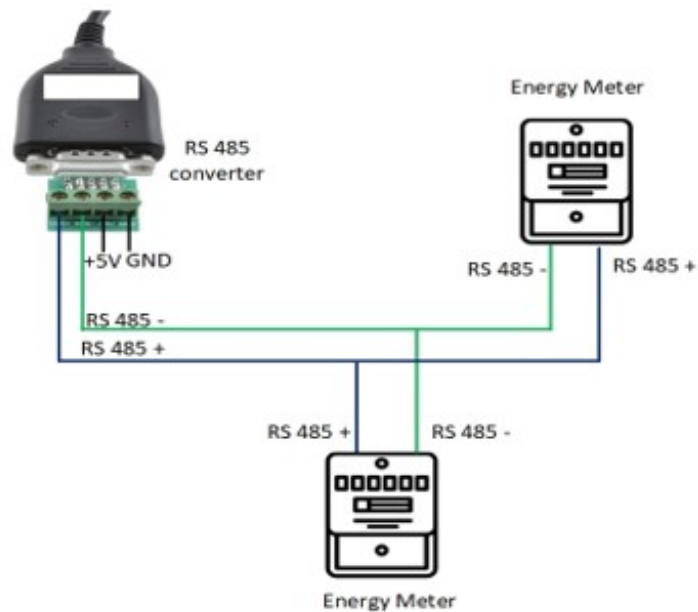


Figure 2.5: RS 485 and energy meter connection

and a database is created inside it. On the micro-controller, script is written, which is serially communicate with the meters using the Modbus RTU protocol.

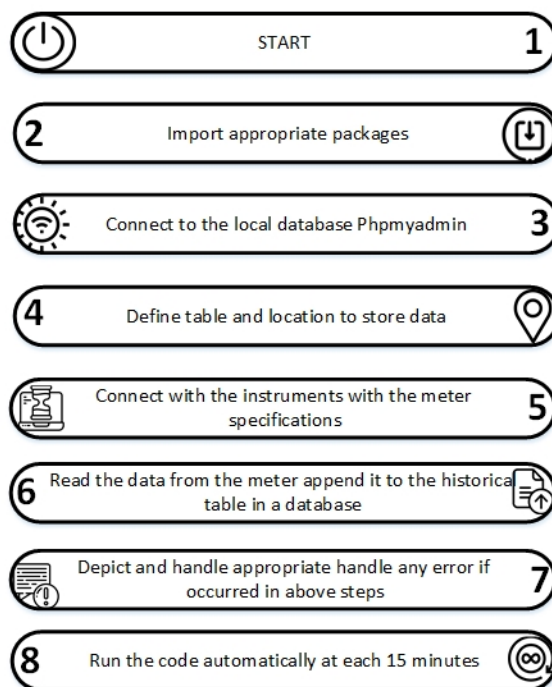


Figure 2.6: Flow diagram for communication with energy meter

A unique slave ID is assigned to every meter of each energy meter. In the case of Modbus, a unique ID of the meter is set by using a Modbus poll software, and it will be permanently stored in the memory of the device. Whenever a query is raised for

communication with an instrument, the device receives the signal, respectively. As all meters have different slave ID and raised query contains meter id, So, it is compared with each meter id, and if it matches, then it will respond. It fetches data from the meter only when a query is raised, which helps to avoid unnecessary communication.

The instrument is connected via a serial port (RS 485), and a USB-to-serial adaptor (RS 485 to USB) should be used at smart agent. For example, we want to communicate Modbus remote terminal mode (RTU) mode, with slave address 1 to which we communicate via serial port number 1.

The following are the recommended steps to be set for communication.

```
instrument.serial.port = minimalmodbus.Instrument('/dev/ttyUSB1', 1)
instrument.serial.baudrate = 9600
instrument.serial.bytesize = 8
instrument.serial.parity = serial.PARITY_NONE
instrument.serial.stopbits = 1
instrument.serial.timeout = 0.05
```

One RS 485 to a USB converter can be use for fetching the data from multiple meters. It works on half-duplex data transmission. It can support a maximum of 32 node information, and more than one devices on the same network are known as the multi-dropping. In this way, we can fetch data. Like, in our application, we are using one RS 485 to USB converter for Peer A. It is fetching and storing the data of all meters shown in Fig. 2.1.

The following command is used to take the value of voltage from the meter.

***voltage = instrument.read\_register(register address, number of decimals=0, functioncode=3, signed=False) [27]***

When the above query is executed, it is reading an integer from one 16-bit register in the slave, possibly scaling it [27]. The slave register can hold integer values in the range 0 to 65535 (“Unsigned INT16”) and -32768 to 32767 (“Signed INT16”).

In the above query of reading voltage, the following terms should be defined.

- *Register address (int)*: It identifies the register which we want to read. The meter manufacturer specifies it and only decimal numbers are allowed.
- *Number of decimals (int)*: Like if meter value is 234 V. and it reads 2340 V. It means it is reading ten times more than original reading, so number\_of\_decimals = 1 will divide that value by ten, and we get only 234 V. Similarly, number\_of\_decimals = 2 will divide it by 100.
- *Function code (int)*: It should be either 3 or 4 for Modbus function.

- *Signed (bool)*: It should be true if we want to get the negative value also. Like, while injecting power into grid or trading to other peer, at that instant power will be negative, so, signed bool should be accurate. If it is False, then it can read any integer range from 0 to 65535. while, if it is true, then it allows negative numbers; also, an integer range is -32768 to 32767. So, if we want reading from a register that can hold negative value also, then we should keep signed as true.

Table 2.4: Modbus Settings

Data type in slave	Signed	Range	Alternative names
INT16(Unsigned)	False	0 to 65535	short
INT16 (Signed)	True	-32768 to 32767	short

The proposed P2P trading platform uses a android application for making the trading process easier. The smart agents present in the peers of the P2P should be properly integrated with this android application for completing a successful P2P trade. Hence, static IP addresses would be provided provided for all the three smart agents present in the proposed model. The android application communicates with this smart agent through node application as shown in Fig.1.2, 2.12, it is required to set up a server on the LAN and run a node application in the smart agent.

So, a static IP address is necessary for the smart agent as we want to use it as a server. The smart agents of the testrig are running on a raspbian operating system, and it has a DHCP client daemon (DHCPD) that allows communication between DHCP and router. DHCP daemon configuration file will enable us to change the PI static IP address in the long term.

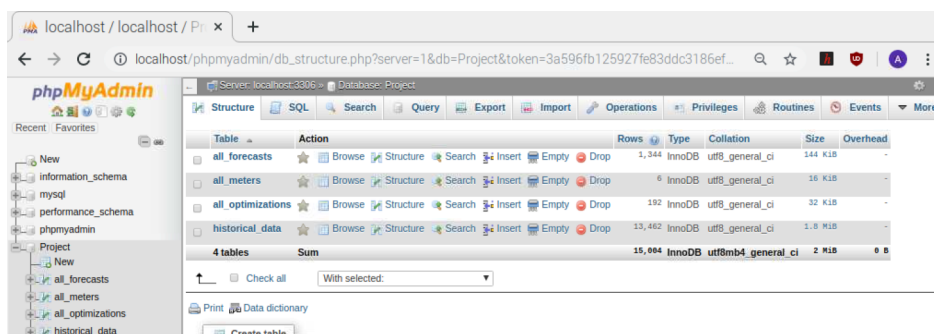
Static IP in the smart agent can be configure by following steps.

- Open the network parameter location by following command.  
*sudo nano /etc/network/interfaces*
- Configure inet static and auto ethernet option and assign the address, netmask, and gateway.
- To configure the static IP, disable the dhcp mode using the following command .  
*sudo systemctl disable dhcpcd*
- Check the static IP by running following command.  
*ifconfig*

## 2.5 Database in Smart Agent

The readings of the energy meter should be stored in a database for load forecasting and scheduling the battery and it is done using the MySQL. The various advantages of using MySQL are the following:

- MySQL is preferred because of its capability to store millions of chunks of data and its data integrity and data accuracy is the key point while managing the data using MySQL database.
- With the database, we have the security groups and privileges to access its data. So, stealing or modification of data is impossible.
- We have the flexibility of updating the data using MySQL.
- Multiple queries can be handled with one table of the database simultaneously. It organizes the data in such a way that it is easy to organize data, sort of data, and interlink two different tables of any database.



The screenshot shows the phpMyAdmin interface for a database named 'Project'. The table 'all\_meters' is selected, and its structure is displayed in a table format. The table has 6 columns and 16 rows. The columns are: 'id' (InnoDB, utf8\_general\_ci, 16 K1B), 'meter\_id' (InnoDB, utf8\_general\_ci, 32 K1B), 'meter\_name' (InnoDB, utf8\_general\_ci, 1.8 M1B), 'meter\_type' (InnoDB, utf8\_general\_ci, 2 M1B), 'meter\_status' (InnoDB, utf8\_general\_ci, 2 M1B), and 'meter\_location' (InnoDB, utf8\_general\_ci, 2 M1B). The table is summarized as having 15,084 rows and a size of 15,084 K1B.

Table	Action	Rows	Type	Collation	Size	Overhead
all_forecasts	Browse Structure Search Insert Empty Drop	1,344	InnoDB	utf8_general_ci	144 K1B	-
all_meters	Browse Structure Search Insert Empty Drop	6	InnoDB	utf8_general_ci	16 K1B	-
all_optimizations	Browse Structure Search Insert Empty Drop	192	InnoDB	utf8_general_ci	32 K1B	-
historical_data	Browse Structure Search Insert Empty Drop	15,462	InnoDB	utf8_general_ci	1.8 M1B	-
4 tables	Sum	15,084	InnoDB	utf8mb4_general_ci	2 M1B	0 B

Figure 2.7: Database in smart agent

As explained in the chapter 1, four different tables are created in the smart agent database. The snapshot of the database is given in Fig. 2.7

1. all\_meter
2. historical\_data
3. all\_forecasts
4. all\_optimizer

The first table of the database is all\_meter table. This table is stores the unique ID's of all energy meters apresent in the system. This ID is reflecting correspondingly in the other tables of the database. A snapshot of the all\_meter table is given in Fig. 2.8.

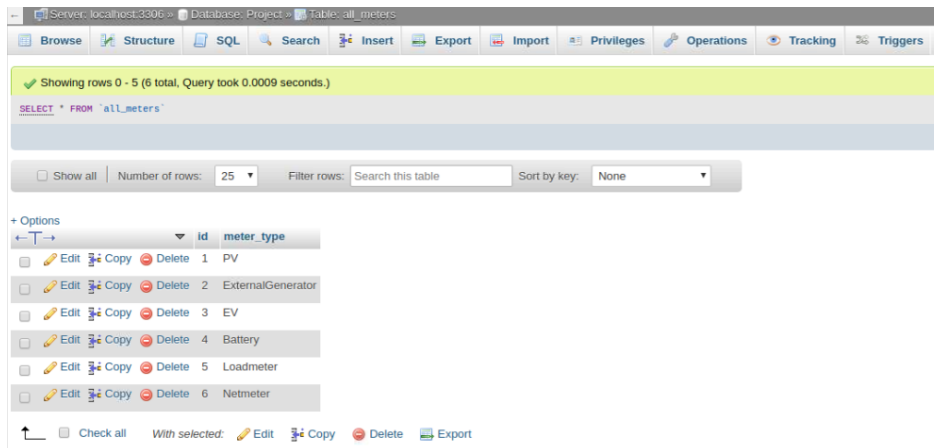


Figure 2.8: All meter table in database

The second table of the smart agent database is the historical data table. Historical data table stores energy meters reading (Power, Energy, SOC of BESS) at every 15 minutes interval. For storing energy meter reading inside the database, we have integrated the database with the python language. The picture of the historical table is attached in Fig. 2.9. In this picture, the `txn_info_1` is the energy readings, and `txn_info_2` is the power reading of the assigned ID's meter.

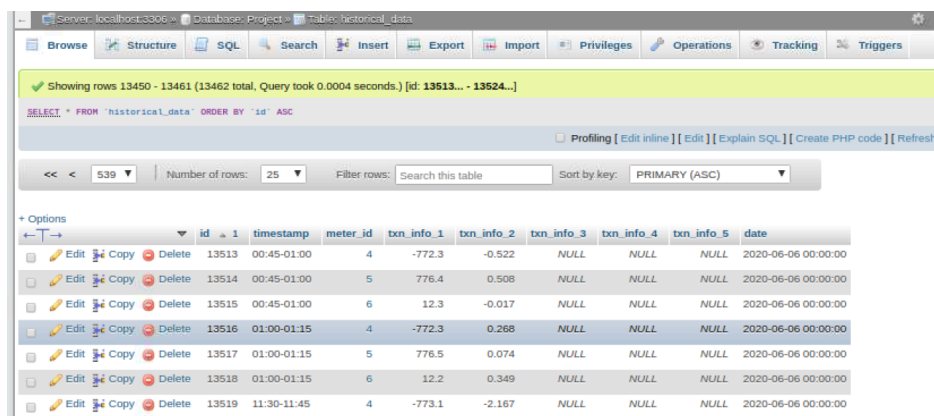


Figure 2.9: Historical data table in database

The third table of the smart agent database is all\_forecast table. The forecasting table is linked with the historical table. The forecasting table provides the estimated values of solar PV and load for next seven days obtained through a linear regression based method. Forecasting is carried out using the previous 30 days data stored in the historical table. Then it is splitting into the training and testing data, and the output of the forecasting code is stored inside the all\_forecasts table of the database. The snapshot forecasting table is attached in Fig. 2.10.

The fourth table of the smart agent database is the all\_optimizer table. It takes input from the all\_forecast table of PV, load forecasting, and solving the optimization

id	timestamp	meter_id	forecast_info1	forecast_info2	price	date
1326	19:15-19:30	5	0.582781	NULL	NULL	2020-06-02 00:00:00
1327	19:30-19:45	5	0.530622	NULL	NULL	2020-06-02 00:00:00
1328	19:45-20:00	5	0.515646	NULL	NULL	2020-06-02 00:00:00
1329	20:00-20:15	5	0.503252	NULL	NULL	2020-06-02 00:00:00
1330	20:15-20:30	5	0.541467	NULL	NULL	2020-06-02 00:00:00
1331	20:30-20:45	5	0.5079	NULL	NULL	2020-06-02 00:00:00
1332	20:45-21:00	5	0.48621	NULL	NULL	2020-06-02 00:00:00
1333	21:00-21:15	5	0.516679	NULL	NULL	2020-06-02 00:00:00

Figure 2.10: Forecasting table in database

formulation. The result of the optimization formulation is stored inside the optimization table. The optimization table is shown in the Fig. 2.11.

id	timestamp	meter_id	forecast_info1	forecast_info2	forecast_info3	forecast_info4	date
53	13:00-13:15	4	1	0	NULL	57	2020-05-27 00:00:00
52	12:45-13:00	4	0	1	NULL	56	2020-05-27 00:00:00
51	12:30-12:45	4	0	1	NULL	57	2020-05-27 00:00:00
50	12:15-12:30	4	0	1	NULL	58	2020-05-27 00:00:00
60	14:45-15:00	4	1	0	NULL	64	2020-05-27 00:00:00
61	15:00-15:15	4	1	0	NULL	65	2020-05-27 00:00:00
73	18:00-18:15	4	1	0	NULL	77	2020-05-27 00:00:00

Figure 2.11: Optimization table in database

## 2.6 Integration of Hardware and Software Layer

The Fig. 2.12 shows integration of the hardware and software layer developed by IIT Gandhinagar and software layer sustain impact team. The node application is running in the smart agent. When the server of the smart agent is running on its assigned port, data from the smart agent pushed into the cloud. The different API's mentioned in the Table 2.5, APIs are posted to get the data into the android application.

### 2.6.1 P2P Trading Steps

The operating steps of the proposed P2P energy trading model is explained with the help of an example below.

Let us consider a power trade between Peer A and Peer B. Both these peers have created an account in the peer energy android application where the user information

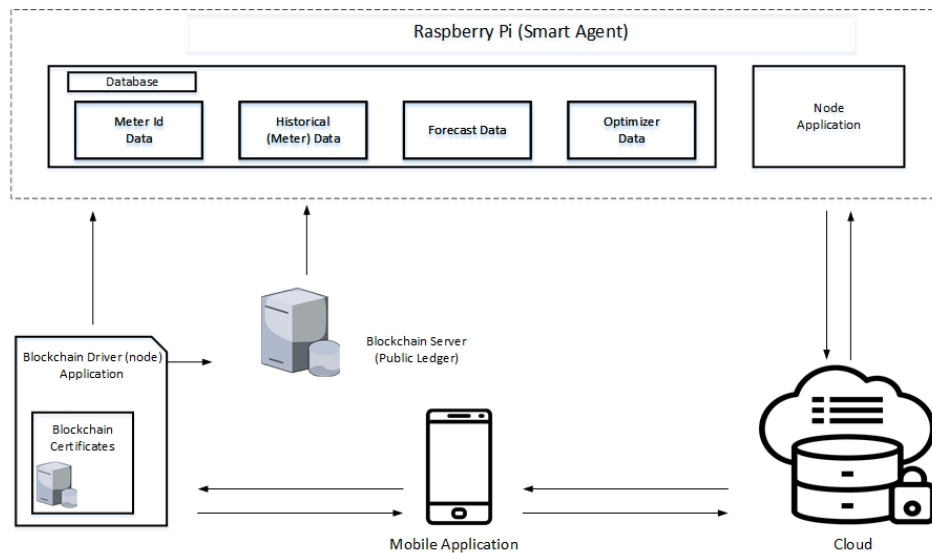


Figure 2.12: Schematic representation of hardware and software layer integration

of the peers are stored. After running the forecasting and optimization algorithms from the android application, it is observed that Peer A has surplus energy of 1 kW between time slots 17:30-18:00. The major steps for trading this power is explained below.

1. Peer A creates a sell bid for this surplus power using the android application.
2. Consumers like Peer B who are looking to buy energy for this time period go through different sell bids and select the most appropriate one. Let us assume that the most economical bid was from Peer A. Hence, Peer A is selected to supply 0.5 units of energy to Peer B for the time period between slots 18:30 - 19:00.
3. The order is confirmed after Peer B makes the payment through the android application and a smart contract is created between Peer A and Peer B using blockchain. It should be noted that the confirmed order cannot be edited but can be cancelled. However, if the bid is not contracted, it can be edited before gate closure time which is 1 hour before the actual trading time.
4. Power flow is triggered between the contracting parties as per the smart contract. The beginning and ending meter readings are used to validate the trade, and if there are any deviations from the smart contract, then penalties are calculated accordingly.
5. If penalties are not present, the order is settled and closed in blockchain.

## 2.6.2 Node Application and Smart Agent

For this trading algorithm to work correctly, the android application should communicate with smart agents. It is achieved through the cloud using a node application. So,

Table 2.5: APIs for Communication with Digital Platform

Functionality	Comments	API
To fetch forecast Information	Used to get information about the PV, Load forecast	/fetchForecastData
To fetch Transaction information	Used to get information of transaction data	/fetchTransactionData
To fetch historical data	Used to get information about meter consumption data	/fetchHistoricalData
To fetch optimization data	Used to get information about the battery scheduling	/fetchOptimizationsData
To check the health of the agent	To check the status of smart agent	/agent/health

when a user uses the android app for update regarding surplus power during a particular time period, a post API request is sent from the mobile application to the smart agent of the respective peer. smart agent checks the request and runs the optimization algorithm. The results of the optimization algorithm are sent back to the mobile application through the node application. A schematic diagram for mobile app and smart agent integration is shown in Fig. 2.12.

First, we make sure that a node is installed in the smart agent. To, check it use the following command.

```
node -version
```

If it is installed, First go into the folder location using the cd/location of folder/ folder name and install node package manager using the following command.

```
npm install
npm -version
```

To make the server up, following commands used.

```
cd/location of folder/ folder name
node server/server.js
```

The message will show that server is running on the port 4012.

The smart agent data export environment is set up with the discussed steps, and after it rest API presented in the Table 2.5 checked with the postman tool to check the smart agent's integration with the adroid application and the blockchain platform.

The Fig. 2.13 shows the API testing result in the postman tool. We are fetching the forecasting data of Peer A. The response is generated in the form of the javascript object notation (JSON) format. These API's mapping the historical, forecasting, and optimization result in the mobile application using this API.



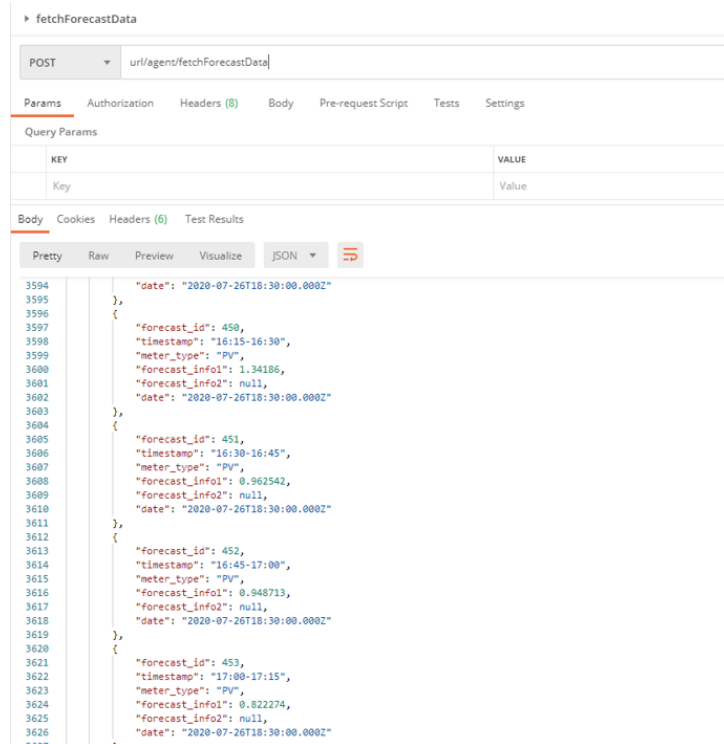


Figure 2.13: Smart agent data in the JSON format in cloud using API

## 2.7 Results and Discussions

The effectiveness of the proposed P2P trading model is validated/checked with the help of a Proof of Concept having three peers at the Water Service Center (WSC-II), IIT Gandhinagar. The electrical layout of the WSC-II is reconfigured such that three peers, i.e., Peer A, Peer B, and Peer C, are created for this purpose.

The formulated algorithm is tested at the testbed shown in Fig. 2.14. The real data from the smart agents database have been taken as the input data of the algorithm. The solar PV and load profile of peer A, B on 27<sup>th</sup> May, 2020 is shown in Fig. 2.15 and Fig. 2.15. The time of use (ToU) [26] and day ahead (DA) electricity price (obtained from the Indian Energy Exchange) of the selected day are depicted in the Fig. 2.16.

Pulp solver in the python language is used to solve the presented energy management algorithm. The specification of Peer A BESS is given in Table 1.1, while Peer B EV battery details have been provided in Table 2.3. Base case and deterministic studies have been performed on the Peer A setup. The minimum and maximum grid power limits tend to infinity.

### 2.7.1 Base Case

In the base case scenario, the highest priority is given to the local loads and BESS. The generated solar power is used to satisfy the energy requirements of the Peer A. If

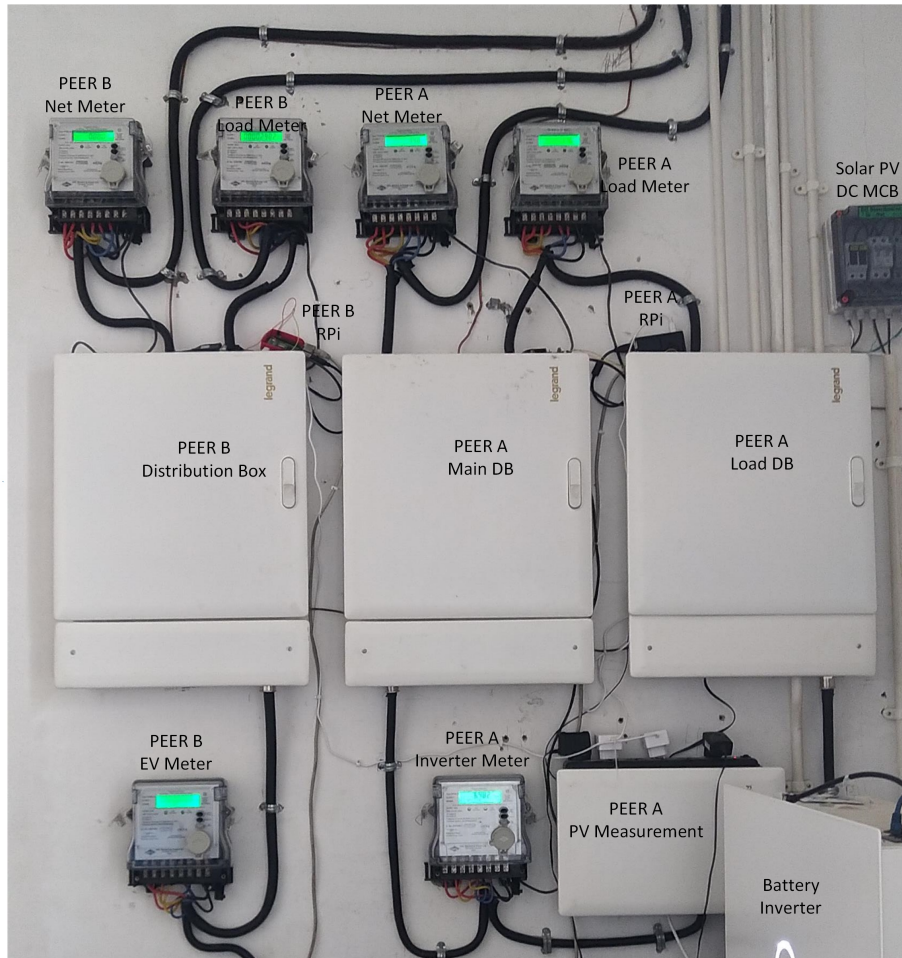


Figure 2.14: P2P trading setup at WSC -II

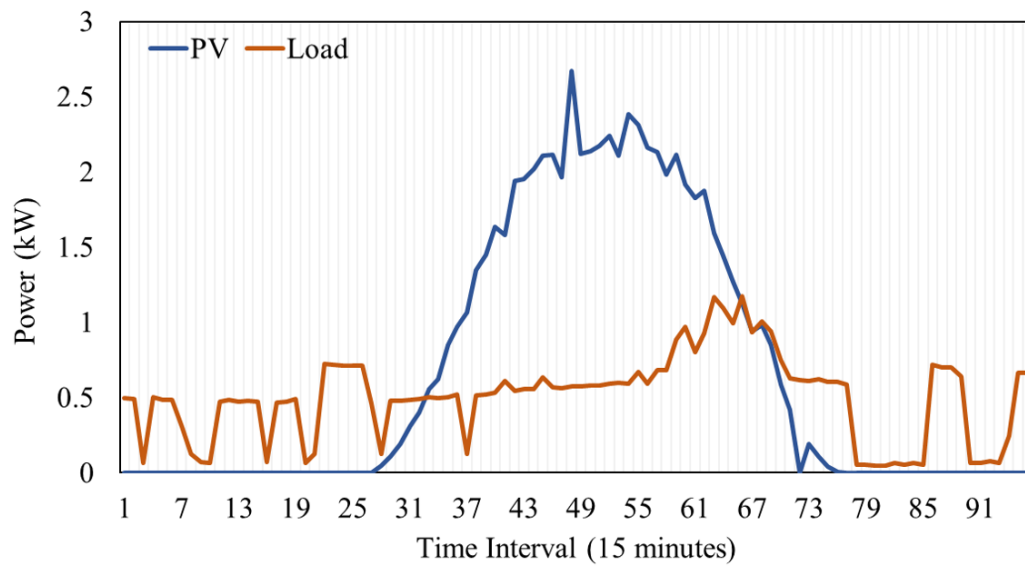


Figure 2.15: PV and load profile of Peer A

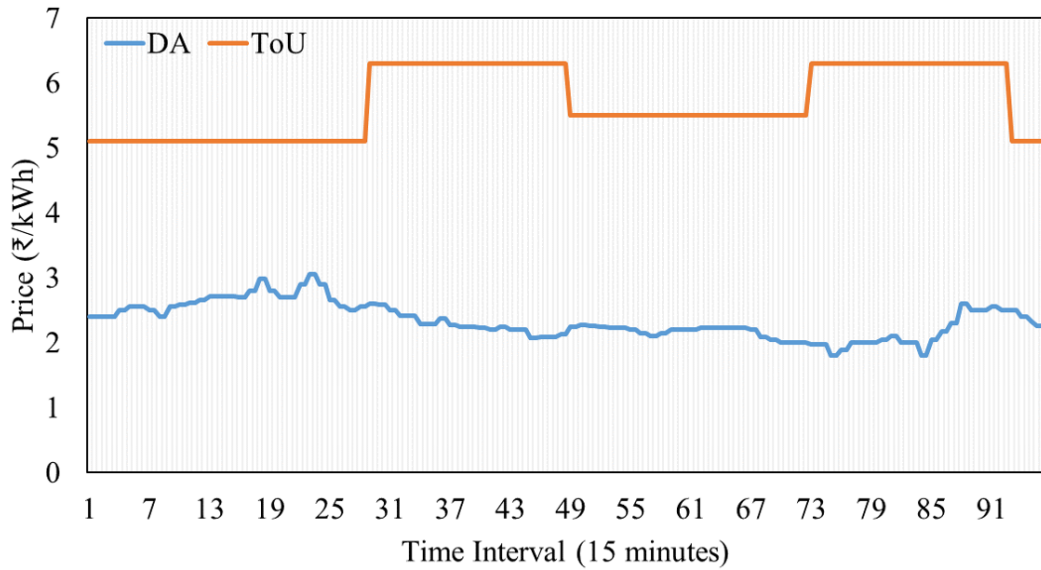


Figure 2.16: Electricity price

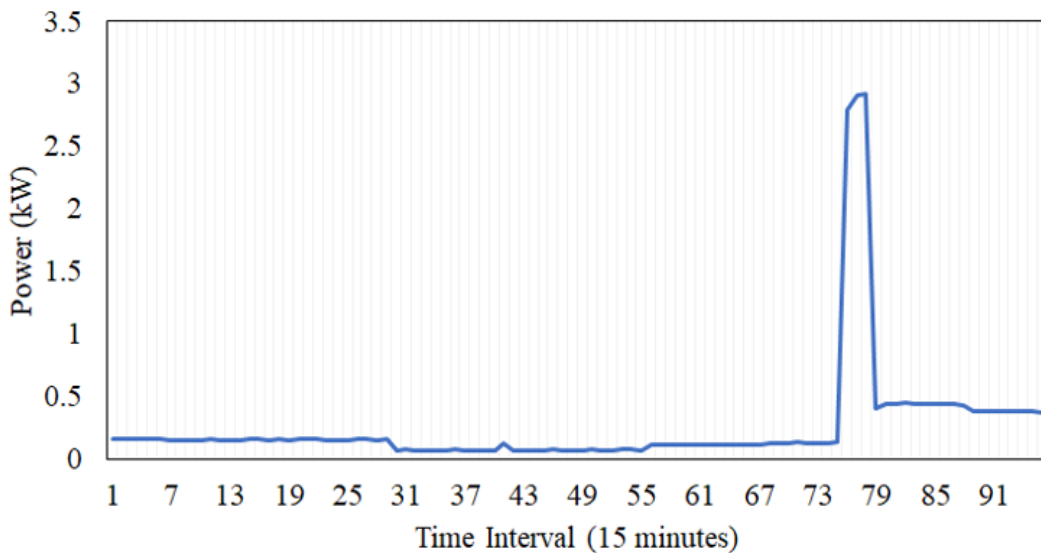


Figure 2.17: Peer B load profile

extra energy is present, the battery is charged to its maximum capacity. The energy is fed back to grid only when the BESS is fully charged and energy requirements of home are satisfied

A local renewable generation has been given the highest priority to meet the load demand. The remaining energy is used to charge BESS up to the  $SOE_{max}$ . The excess power then feeds into the grid. When load demand exceeds the solar PV power at that time, BESS starts delivering partial power up to  $SOE_{min}$ , and the remaining power is brought from the grid. It should be noted that BESS discharge in base case depends on

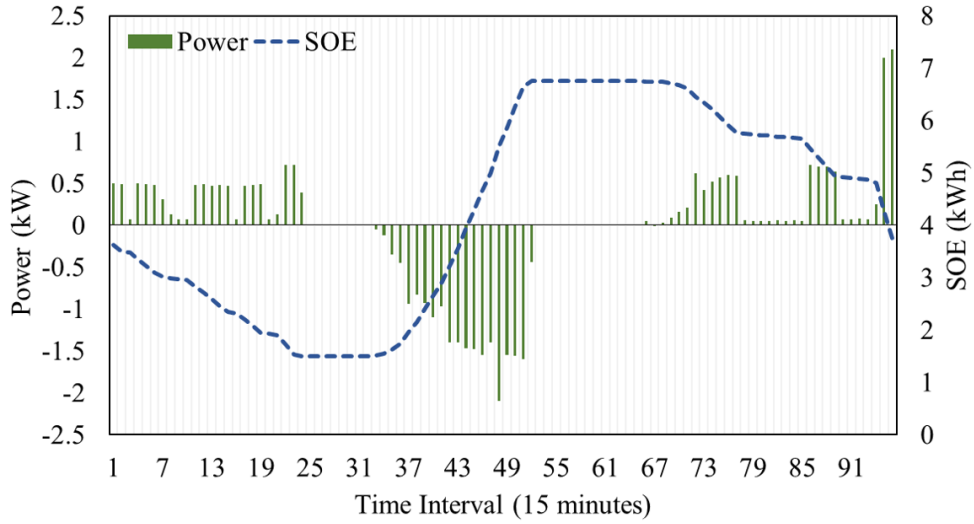


Figure 2.18: BESS power dispatch & SOE (case 1)

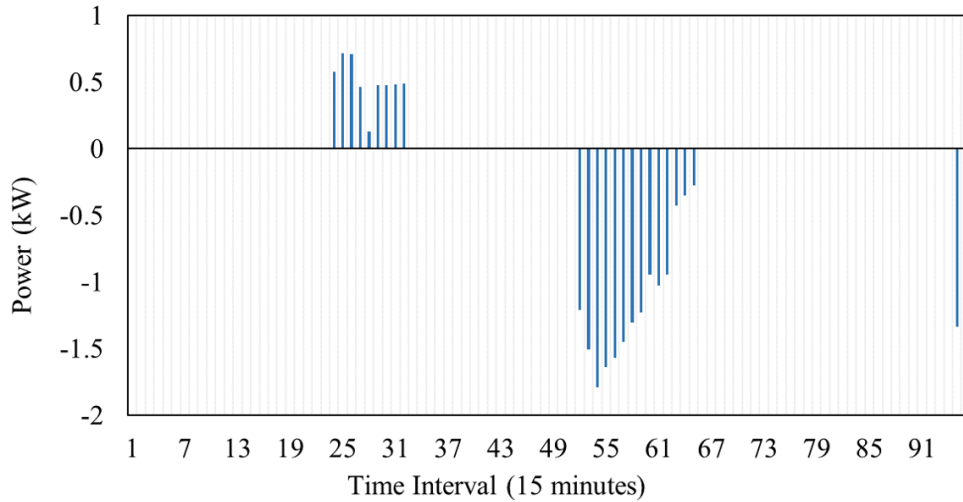


Figure 2.19: Grid power dispatch (case 1)

availability of extra power, and independent from the electricity price signal.

Grid dispatch and BESS and SOE dispatch for the base case are provided in Fig. 2.19, 2.18 respectively. It is observed from the schedules that BESS is charged to  $SOC_{max}$  during the day time between 33<sup>rd</sup> time interval to 53<sup>rd</sup> time interval, when the solar PV power generated is more than the load. After the BESS is fully charged it supplies power to the load during time interval 67<sup>th</sup> to 96<sup>th</sup>, when the solar PV generation is less than the load. The electricity price is not taken into account for BESS scheduling. Ideally, it should discharge in the peak tariff period to avail of the maximum economic profit.

## 2.7.2 Deterministic Case

In this case, the scheduling of BESS is obtained through an optimization algorithm where forecasted values of load demand and solar PV power along with electricity price provided as input. The Time of Use (ToU) tariff price [26] and day ahead price obtained from the IEX is shown in 2.16. In this case, we are assuming no uncertainty in the forecasted values. Hence it is considered a deterministic case.

BESS scheduling is done separately for DA and ToU tariffs. From Fig. 2.20 of BESS DA scheduling, it is clear that BESS is discharged while the tariff is high in the 17<sup>th</sup> to 19<sup>th</sup> and 22<sup>nd</sup> to 25<sup>th</sup> timeslot. It is discharged in the 49<sup>th</sup> to 53<sup>rd</sup>, 62<sup>nd</sup> to 63<sup>rd</sup>, and 88<sup>th</sup> to 93<sup>rd</sup> timeslot due to a higher price in that duration. It is charging in the timeslots when the price is low. It minimizes the power drawn from the grid during peak tariff rates and provide more economic benefits to the consumer.

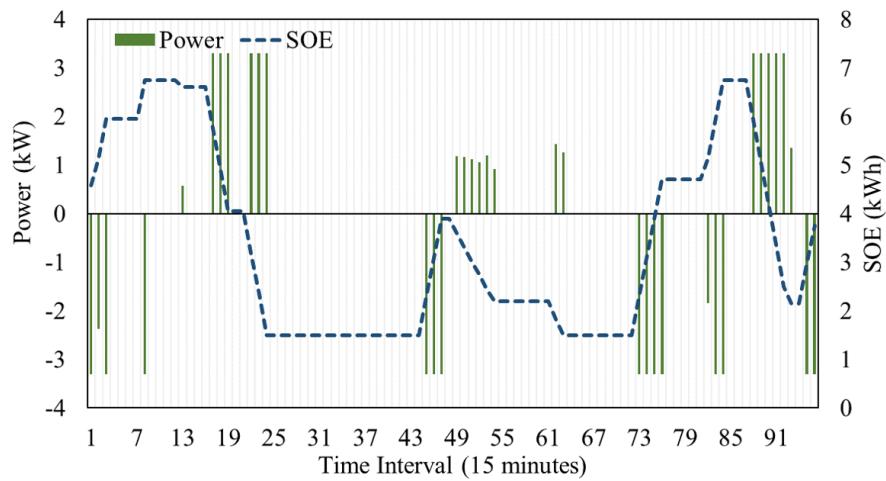


Figure 2.20: BESS power dispatch & SOE (case 2 DA tariff)

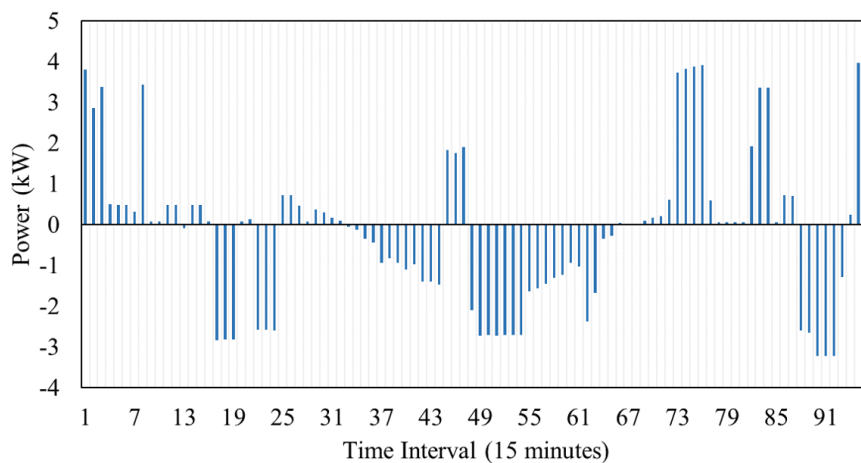


Figure 2.21: Grid power dispatch (case 2 DA tariff)

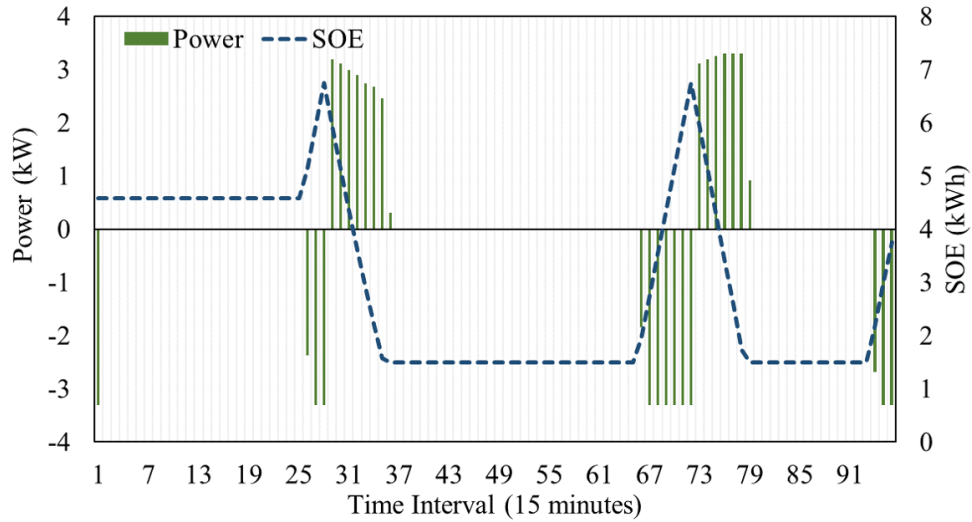


Figure 2.22: BESS power dispatch & SOE (case 2 ToU tariff)

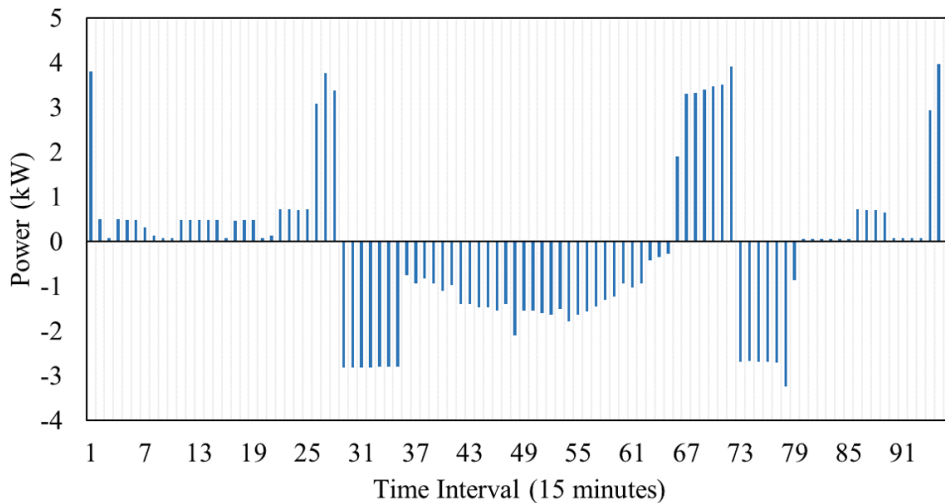


Figure 2.23: Grid power dispatch (case 2 ToU tariff)

From the Fig. 2.22 of BESS scheduling based on the ToU tariff, we can see that it is discharging in timeslot from 29<sup>th</sup> to 35<sup>th</sup> and 73<sup>rd</sup> to 79<sup>th</sup> to gain the maximum price for grid fed power. ToU tariffs during those durations are high. However, it is charging in the timeslot 1<sup>st</sup>, 25<sup>th</sup> to 28<sup>th</sup>, 66<sup>th</sup> to 72<sup>nd</sup>. BESS is charged in the 93<sup>rd</sup> to 96<sup>th</sup> timeslot to maintain its SOE equal to initial SOE. During charging schedules, we can see low tariffs in those durations. So, power is reduced during peak tariff intervals, and it increases the benefit to the consumer. A Table 2.6 giving the comparison of test case 1 and case 2 is described.

Table 2.6: Comparison Between Base Case and Deterministic Case

	Base Case		Deterministic Case	
	DA	ToU	DA	ToU
Total Cost (INR)	-7.26	-18.73	-12.16	-32.44
Electricity purchased (kWh)	1.12	1.12	15.35	15.14
Electricity sold (kWh)	4.60	4.60	18.69	18.58
Net Electricity (kWh)	-3.47	-3.47	-3.33	-3.44
Energy from BESS (kWh)	5.16	5.16	11.88	10.18
Energy to BESS (kWh)	5.41	5.41	12.60	10.79
BESS cycle	0.7	0.7	1.62	1.39

### 2.7.3 P2P Energy Trading

A P2P energy trade between Peer A and Peer B is explained in this section. The load profile of Peer B on 27<sup>th</sup> May, 2020 is as shown in Fig. 2.17. Peer B load is the WSC II compressor pump and the drainage pump, and it is observed that the load is constant for most part of the day except for the time interval between 77<sup>th</sup> to 79<sup>th</sup>, when the pumps are operated.

Peer A has solar PV power and BESS as a energy resources. Peer B has a load demand in the 77<sup>th</sup> to 79<sup>th</sup> slots hence it is looking for energy seller can meet his demand on android application. Peer A earlier created a sell order for that duration on peer energy android application. Peer A can sell its power to Peer B in that duration at a more competitive price than the grid tariff and FiT. Peer B agrees on that bid post by Peer A on the android application as shown in Fig. 2.24 and successful execution of trade increases social benefit of Peers. Fig. 2.24 trade is created between Peer A and Peer B to deliver a 1 unit of energy from 18:30 to 19:00. At 18:30 PM, Peer A starts delivering 2 kW of power, as depicted in the Fig. 2.25. At the completion of the trade, from the smart agent database to the blockchain and mobile application, and the transaction details of the trade is store in the blockchain node.

At the beginning of the trade, a post request API from the digital infrastructure is send to the smart agent. The node application running in the smart agent responding to the post API and sends data from the historical data table at the start of the trade. At the completion of trade, node application again responding to a post request API sent by android application.

Here, from the Fig. 2.25, it can be observed that Peer A delivering 2 kW of power during energy trade. The transaction details of the trade is shown in Fig. 2.26 and it is containing the information regarding the the energy meter readings (Power and Energy) of the Peer A and Peer B at the start and the end of the trade. From Fig. 2.26, it can be inferred that Peer A energy meter reading at the start of the trade was -666.8 and at the end of trade was -667.9. So, Peer A fed 1.1 units of energy during that time. Similarly, buyer Peer B consumes only 0.1 unit (271.1 - 271).

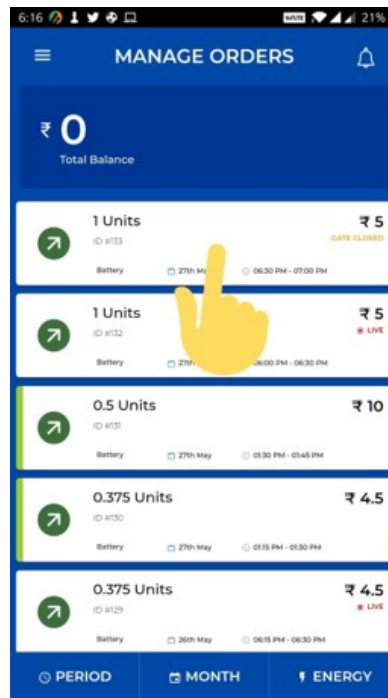


Figure 2.24: Trade creation in the android application

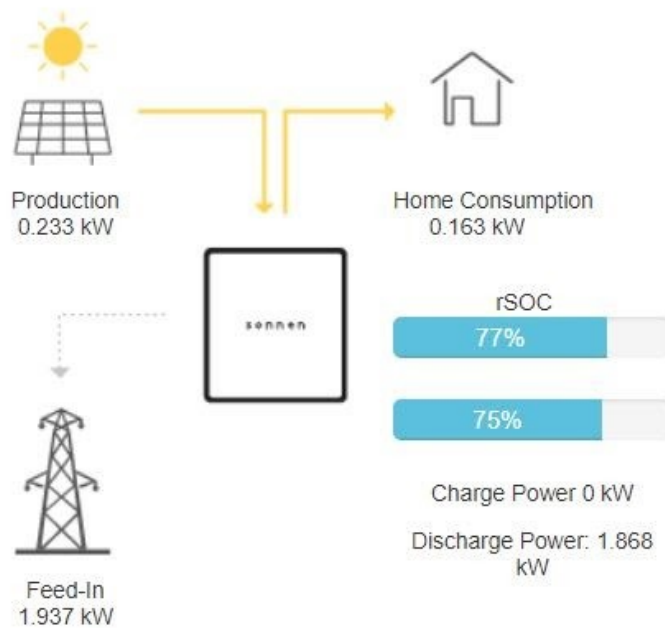


Figure 2.25: Battery status during energy trading

Here, the benefit was in terms of price. Let's say, as per DA tariff rate, if Peer A was injecting power into the grid, he would have got 2.3 INR, but as he delivered power to Peer B at 5 INR and benefited by 2.7 INR provided Peer B consumed all the power delivered by Peer A



```

11     "ENERGY": 1,
12     "TIME_FROM": "2020-05-27 18:30:00.0",
13     "TIME_TO": "2020-05-27 19:00:00.0",
14     "LOCATION": "hyderabad",
15     "AMOUNT_OF_POWER": 2,
16     "PRICE": 5,
17     "TRADE_S_TIMESTAMP": 1590584702896,
18     "TRADE_C_TIMESTAMP": "",
19     "TRADE_STATUS": "TRADING_COMPLETED",
20     "Seller_METER_READING_S": -666.8,
21     "Seller_METER_READING_E": -667.9,
22     "Buyer_METER_READING_S": 271.1,
23     "Buyer_METER_READING_E": 271.1,
24     "B_FINE": 0,
25     "S_FINE": 0,
26     "TRADE_E_TIMESTAMP": 1590586502866
27 }

```

Figure 2.26: Blockchain smart contract with transaction details

## 2.8 Summary

A P2P energy trading platform utilizing the blockchain technology for transaction validation is proposed in the chapter. The proposed model required forecasted values of solar PV and load for accurately scheduling the battery, which was obtained a linear regression-based method. The ICT framework for energy trading before and after a trade is also presented in the chapter. The smart agent data management using MySQL and phpMyAdmin is also discussed. The energy management algorithm is used for minimization of the purchasing electricity cost from the grid. The effectiveness of the proposed case studies has been validated on the tested. The testing of the P2P energy trade is also discussed in the chapter. From these experiments, it is observed that the proposed model can effectively trade the energy among these peers without the aid of a central control unit. The next chapter will discuss the power electronics converter and the control strategy for achieving the vehicle to grid discharge as per obtained schedules from the Peer B energy management formulation.

## Chapter 3

# Grid Connected Bidirectional Converter

EV and rooftop PV systems with battery energy storage systems (BESS) reduce carbon footprints and greenhouse gas emissions. Peer to Peer (P2P) energy trading platform at IIT Gandhinagar have two prosumers and one consumer. Peer B in the testbed has an EV, it can be discharged into grid to meet energy demand of other peers. Energy management algorithm discussed in chapter 2 gives the optimized schedules of the EV battery. The obtained schedules play a role in discharging a battery to gain the maximum profit. It can be achieved by a robust control strategy of the power electronic converter, which helps in achieving the targeted active power flow in the grid. Hence, the chapter focuses discussion on the control strategy of the power electronics converter to achieve scheduled power flow for the EV.

### 3.1 Introduction and Literature Survey

Deployment of distributed generation technologies, such as solar PV and V2G of an EV, has played a significant role in converting traditionally passive consumers into prosumers to manage their storage, production, and usage of energy optimally. The Paris declaration on Electric Vehicles (EVs) and climate change is a crucial element to the shift from bio-fuel-based vehicles to EVs that aims to deploy 100 million EVs worldwide by 2030 [1].

A comprehensive review of different EVs, plug-in hybrid electric vehicles (PHEVs), and its V2G capability with power electronics strategies have been carried out in [28]. Review work on V2G technology, including different EV charging strategies and its effect on the distribution grid, has been carried out in [29]. A case study using the inverter DC link capacitor to mitigate the reactive power is provided in [30], and the impact of V2G on the battery is also carried out in it.

Smart charging is a series of intelligent functionalities to control the charging power to create a flexible, sustainable, low cost, and efficient charging environment and it is an excellent asset in the grid because of its capability to change the power and the ability of both charging as well as discharging. Dynamic EV charging based on the

residential load and the solar PV generation can be done with the help of the smart charger developed in [31], in collaboration by Cohere. However, due to limitation of bi-directional chargers, the potential of discharging battery is not used at an extensive level.

The integrated power train traction and converter topology to have bidirectional flow between vehicle and grid have been discussed in [32]. Renewable energy integration into the charging infrastructure and comparison of the different converter topologies for the EV charging also addressed in [33]. Frequency regulation can be performed by charging the EVs batteries when generation exceeds the load demand and by discharging them when load demand exceeds generation. V2G systems can contribute to frequency regulation to fine-tune the frequency and grid voltage by matching generation to load demand. The demonstration of V2G for frequency regulation from an EV has been carried out in [34]. Work on the hierarchy frame for the V2G application and the mathematical model for smart charging with grid constraints are carried out in [35]. The opportunities and the difficulties in achieving the bidirectional power flow between grid and vehicle have been discussed in the [36]. The smart charging, battery technologies, standards, and infrastructure for the successful V2G operation have been addressed in the [37]. It also gives information on the communication and control between the vehicles and the grid operator. The work for measuring the power losses of a grid-integrated vehicle system in detail has been carried out in [38]. The different charging standards for implementing V2G and dynamic charging, using the CCS Combo and Chademo for different EVs has been discussed in the [39]. Currently, charging of an EV is an uncontrolled process where the EV plugged to the charger at a fixed power and charges until the SOC is 100%. Smart charging increases the flexibility of charging by controlling the charging power and charging power flow direction [1], [23].

The economic analysis and financial return for the consumers of the V2G technology have been carried out in [40]. The rapid growth of V2G networks will increase the distributed storage capacity significantly. Also, V2G can support abundant scale RES and benefit both the system operators and vehicle owners.

## 3.2 Vehicle to Grid (V2G)

The EV battery rating considered in this chapter is 19.2 kWh. Most of the time, EV remains in static mode, we can utilize this battery for feeding the power into the grid whenever the tariff is high. This concept of utilizing the battery power for the ancillary services is known as the V2G regulation. However, this happens with a higher level of communication.

The block diagram 3.1 shows the EV with a lithium-ion battery of 19.2 kWh. It can facilitate the V2G feature like during a high tariff, and an EV owner can discharge part

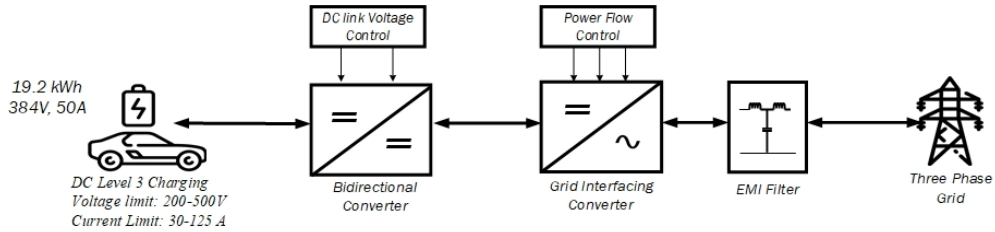


Figure 3.1: [ Block diagram of the V2G mode of operation of an EV]

of its battery power to support the grid. Block diagram also includes the power electronics converter to control the power flow, filters to reduce losses component of current and the control strategies. EV battery is interfaced with the grid using a bidirectional DC-DC converter and the DC-AC voltage source converter.

### 3.3 Battery Discharging Characteristics

Following parameters are reflecting the battery behaviour in practical condition.

- Nominal voltage ( $V_{nom}$ ): The rated voltage of a battery during fully charged state is known as  $V_{nom}$ . When a load is connected to battery, it is gradually reduced to a battery voltage.
- Nominal current ( $I_{nom}$ ): The rated current of a battery during charging or discharging state is known as  $I_{nom}$ . Typically, the battery discharging current is less than or equal to  $I_{nom}$ .
- C rate: It is the charge or discharge rate of a battery. It is defined as the amount of current drawn from or fed in to the battery, divided by the nominal ampere-hour capacity of the battery.

Fig. 3.2 shows the behaviour of the battery voltage corresponding to the different discharge rates. From Fig. 3.2 we can see that there is a reduction in the battery voltage with the increased discharge currents. Battery charge and discharge capacities are always lying between upper and lower cut-off voltages. It can be seen by the nominal voltage region in the 3.2.

The battery characteristics curve is shown in Fig. 3.9. It can be inferred from Fig. 3.9 that battery operates in three regions. The first region is the exponential voltage drop; it is when the battery is charged, and its width depends on the battery type. The second region is the voltage drop of the battery due to the extraction of charge until the voltage reaches the nominal value. The third region is the full discharge of the battery and depicts the rapid drop in voltage.

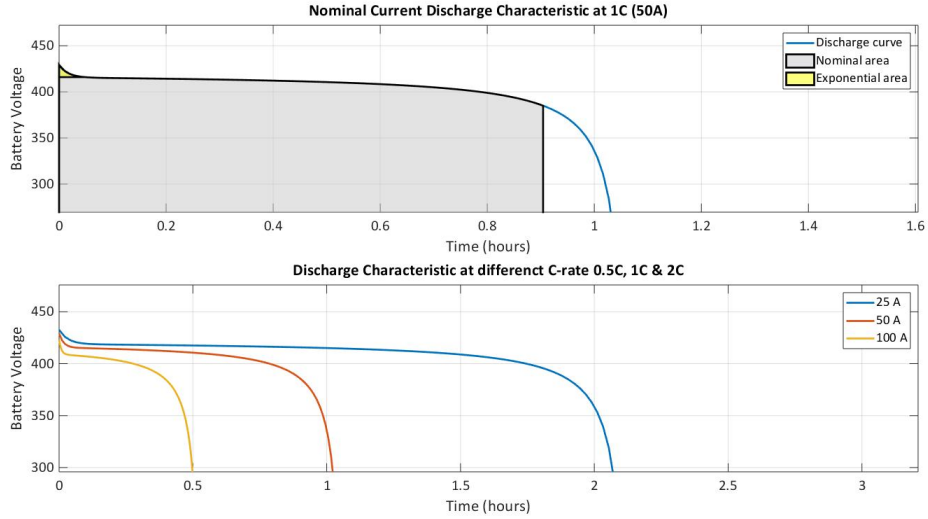


Figure 3.2: Battery discharging behaviour to different C rates

Battery discharging at the 2 C rate, can discharge in around half an hour, while at the 0.5 C rate, it can discharge for two hours. A higher C rate leads to higher energy losses due to the internal resistance of a battery. During acceleration and the hill-climbing, an EV battery has to deliver higher C current.

### 3.4 Methodology : Battery Power Flow Control

The grid-connected EV with power electronics circuitry is shown in Fig. 3.1. The DC link voltage required depends on the maximum line to line voltage. For, three-phase, it is calculated from (3.8). Hence, the DC-DC bidirectional converter steps down the voltage in charging mode and increases in the discharging mode of the battery. It adjusts EV battery voltage to the dc-link voltage, which is necessary for grid interfacing inverters to produce the sinusoidal voltage at the grid voltage value during V2G mode of operation.

The DC-DC bidirectional converter operates in such a way that DC link voltage is constant and maintains the desired current flow controlled by DC-AC converter. It observes the dc-link voltage and battery current using appropriate sensors and compare them with the reference value and accordingly adjusts the duty cycle of the DC-DC bidirectional converter. The control strategy of the DC-DC bidirectional converter is shown in Fig. 3.4. The outer control loop regulates the DC link voltage constant using a PI controller, and the inner PI controller is used to control the current to enhance dynamic performance. For the control of three-phase three-leg Voltage source Converter (VSC), the synchronous reference frame (SRF) concept is implemented here.

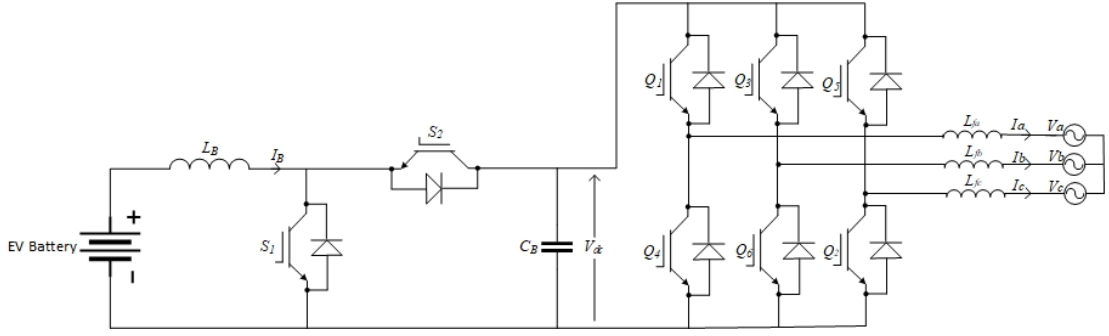


Figure 3.3: Grid integration of EV battery

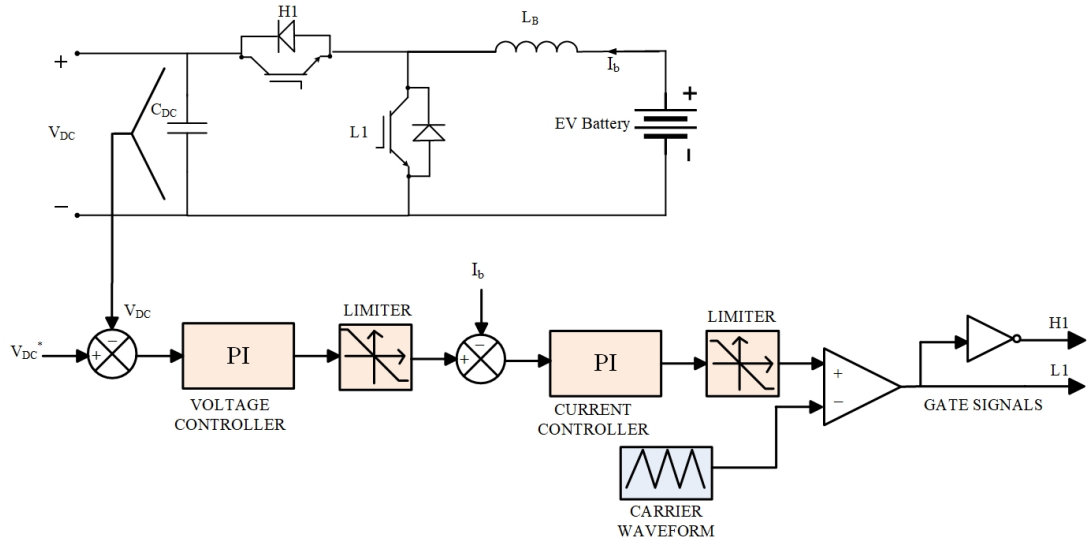


Figure 3.4: Control strategy of DC-DC bidirectional converter

Park transformation is used for converting the three-phase time domain component in abc reference frame into the synchronously rotating dq0 frame. The d-q frame has direct, quadrature, and the zero axis component but zero axis component is neglected due to its zero value. The transformation from the synchronously rotating d-q reference frame to the three-phase time domain component abc is the inverse of park transformation. The following equations show the park and inverse park transformation.

By using park transformation, three-phase currents are converted into the dq0 currents as described in (3.1).

$$\begin{bmatrix} i_d \\ i_q \\ i_0 \end{bmatrix} = \frac{2}{3} \begin{bmatrix} \cos \theta & -\sin \theta & \frac{1}{2} \\ \cos(\theta - 2\pi/3) & -\sin(\theta - 2\pi/3) & \frac{1}{2} \\ \cos(\theta + 2\pi/3) & \sin(\theta + 2\pi/3) & \frac{1}{2} \end{bmatrix} \begin{bmatrix} i_a \\ i_b \\ i_c \end{bmatrix} \quad (3.1)$$

The PCC voltage and load currents are sensed and used as the feedback signal, as shown in Fig. 3.6.

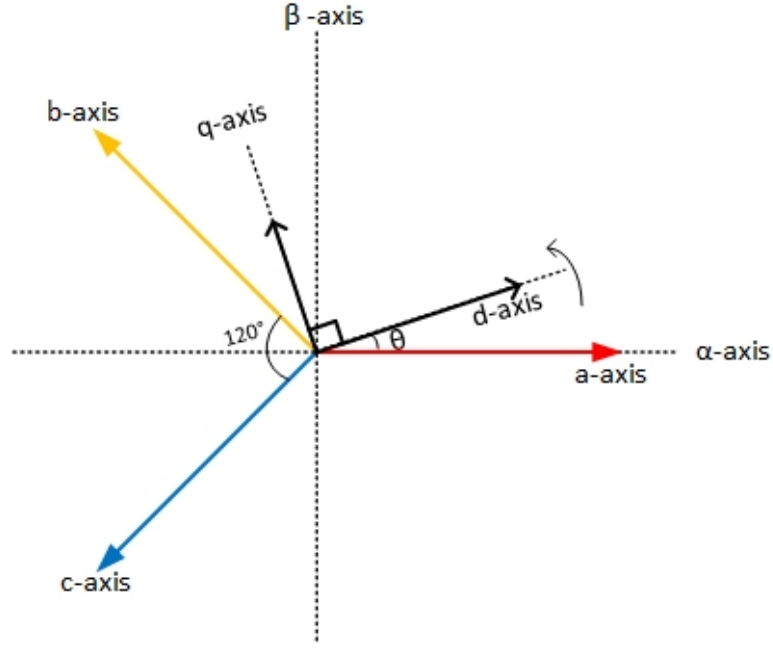


Figure 3.5: Park transformation

The d-axis current containing the two components.

1. Fundamental active current component ( $\bar{i}_d$ )
2. Oscillating active current component ( $i_{dl}$ )

$$i_{Ld} = \bar{i}_d + i_{dl} \quad (3.2)$$

Similarly q-axis current containing the two components.

1. Fundamental reactive current component ( $\bar{i}_q$ )
2. Oscillating reactive current component ( $i_{ql}$ )

$$i_{Lq} = \bar{i}_q + i_{ql} \quad (3.3)$$

Three Phase PLL, as shown in Fig. 3.6, is used continuously to synchronize the grid voltage frequency [26]. It is used to detect if there is any mismatch in the grid interfacing converter and the grid frequency, as it can lead to the large circulating current in the grid interfacing converter and damage the power electronics components. The PLL tracked frequency is used to set the frequency of the grid interfacing converter by controlling switching pulses. The  $I_d$  and  $I_q$  consist of the fundamental and harmonic components. Synchronous reference frame extracts useful DC quantities by a low pass filter (LPF), as shown in Fig. 3.6. The LPF is used after the park transformation to extract the DC component of  $I_{Ld}$  and  $I_{Lq}$ , in this way the harmonics components are separated from the  $I_{Ld}$  and  $I_{Lq}$ .

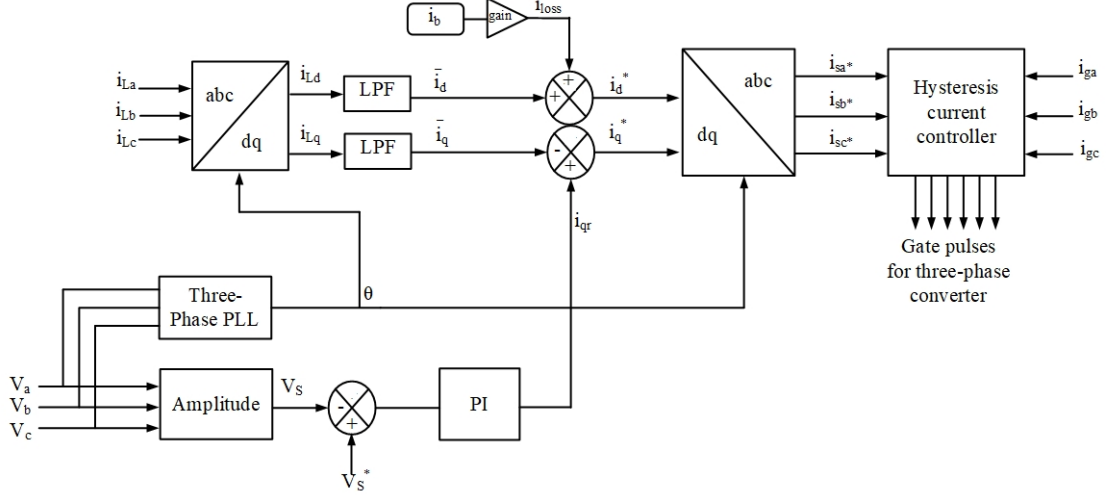


Figure 3.6: Control strategy of grid connected bidirectional converter

The reference currents ( $i_d^*$ ,  $i_q^*$ ) are obtained by adding the active power component and the current loss component ( $i_{loss}$ ) where current ( $i_{loss}$ ) is inferred from the desired current flow of the battery.

$$i_d^* = \bar{i}_d + i_{loss} \quad (3.4)$$

$$\begin{bmatrix} i_{sa}^* \\ i_{sb}^* \\ i_{sc}^* \end{bmatrix} = \frac{2}{3} \begin{bmatrix} \cos \theta & \sin \theta & 1 \\ \cos(\theta - 2\pi/3) & \sin(\theta - 2\pi/3) & 1 \\ \cos(\theta + 2\pi/3) & \sin(\theta + 2\pi/3) & 1 \end{bmatrix} \begin{bmatrix} i_d^* \\ i_q^* \\ i_0^* \end{bmatrix} \quad (3.5)$$

The current should be in phase with the PCC voltage, and the zero sequence component of the current should be zero. The inverse park transformation is shown in the (3.5) where quadrature component of source current should be zero as the reactive component of current must be zero, while  $i_{sa}^*$ ,  $i_{sb}^*$ , and  $i_{sc}^*$  are the reference currents.

The PI controller is used for maintaining the reference voltage at the grid side PCC terminal voltage to achieve zero voltage regulation (ZVR). Its output is assumed as the reactive current component of the current  $i_{qr}$ , and  $i_q^*$  is obtained by the difference of the quadrature axis component of the current  $i_{qr}$  and the  $\bar{i}_q$ . To achieve the ZVR mode of VSC, supply must deliver the reference current  $i_d^*$  and the  $i_q^*$ .

The AC terminal voltage at PCC calculated by,

$$V_s = \sqrt{2/3} \sqrt{(V_a^2 + V_b^2 + V_c^2)} \quad (3.6)$$

The amplitude of AC voltages at PCC is computed from the  $V_a$ ,  $V_b$ , and  $V_c$  as per (3.6) where it is subtracted from the peak amplitude of line to line voltage and given



to the PI controller to obtain the reactive current component. The reference quadrature axis current is calculated as per (3.7). By using reverse Park transformation, a three-phase supply current is obtained from the  $i_d^*$  as in (3.5),  $i_q^*$  as in (3.7) and  $i_0^*$  is set as zero.

$$i_q^* = i_{qr} - \bar{i}_q \quad (3.7)$$

### 3.4.1 Hysteresis Band Control

The current controller of the three-phase voltage source converter (VSC) influences the entire control structure. There are numerous methods available for it, such as Hysteresis current control, PWM control, predictive control, linear proportional integration method. Hysteresis current controller is utilized here, as the controller controls each phase independently, and generates PWM switching pulses for the VSC. It uses the bang-bang instantaneous control technique, in which compensation current is compared with the reference current within a specified band. In the hysteresis band control, reference wave has an upper band and a lower band. The actual current lies in this entire band.

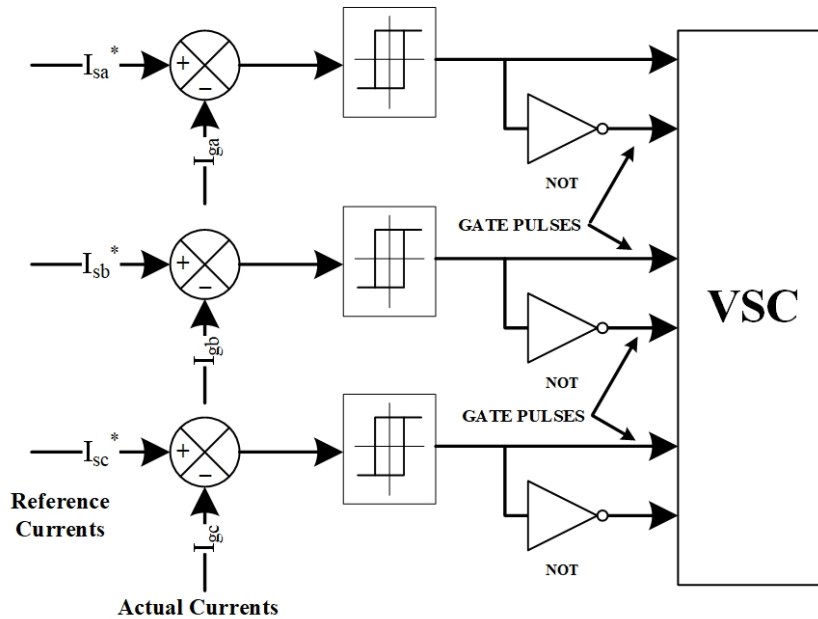


Figure 3.7: Hysteresis current controller

## 3.5 Results

The performance of the aforementioned power electronics control strategy is verified by simulating the complete system in the Simulink environment of MATLAB. A Lithium-ion battery with a nominal voltage of 384 V, DC voltage range 336-432 V, and a nominal capacity of 50 Ah has used in the simulation. The total simulation time is set to 5 seconds and described as per 3.1.

Table 3.1: Battery Current References

Time (s)	Battery State	Battery Current (A)
0 - 1	Discharging at 1 C rate	50 A
1 - 1.5	Idle	0 A
1.5 - 2.5	Charging at 0.5 C rate	-25 A
2.5 - 4	Discharging at 0.5 C rate	25 A
4 - 5	Idle	0 A

Fig. 3.8 shows the EV power available on the grid side. In Fig. Positive values represent 3.8 discharging of an EV battery, while negative values of the current represent the charging.

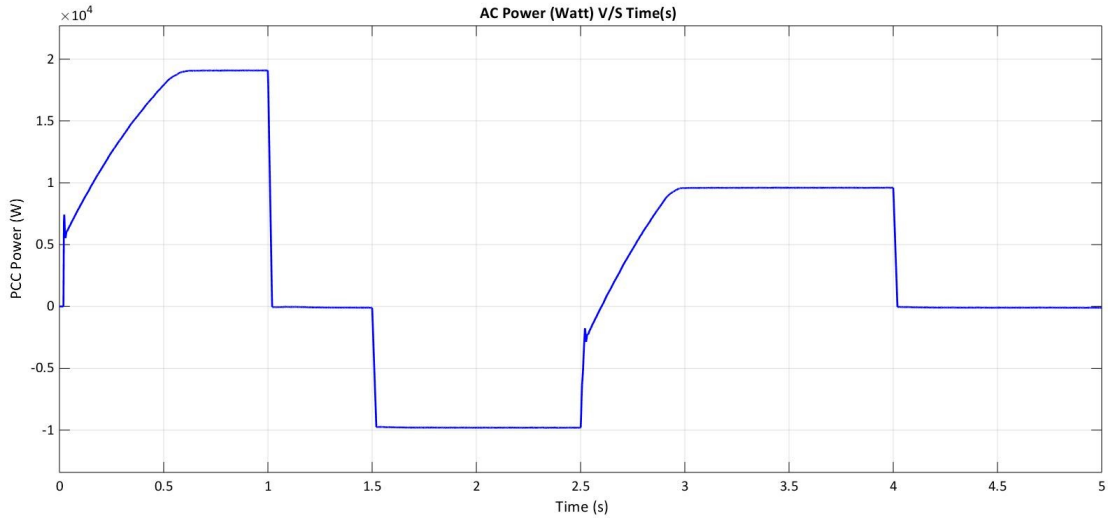


Figure 3.8: Active power dispatch to grid

The DC link voltage should be nearly equal to 700 V. It is calculated from the 3.8, where  $m$  is defined as a modulation index.

$$V_{DC} = \frac{2\sqrt{2}}{\sqrt{3}m} V_{line} \quad (3.8)$$

The DC link voltage is on the stepped upside of the boost converter and maintained at 700 V by the DC-DC bidirectional converter as in Fig. 3.4.

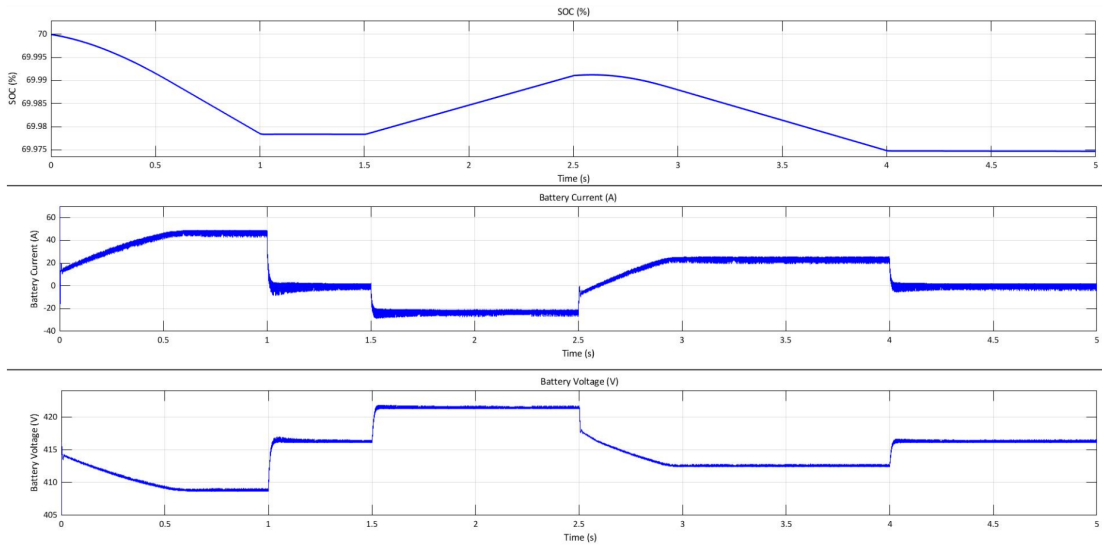


Figure 3.9: SOC, battery current & battery voltage

The battery parameters SOC, current and voltage of an EV battery on the DC side are depicted in Fig. 3.9 as it is showing the battery behaviour as per given commands. The change in the SOC and voltage of the battery is as per the different C rates of current.

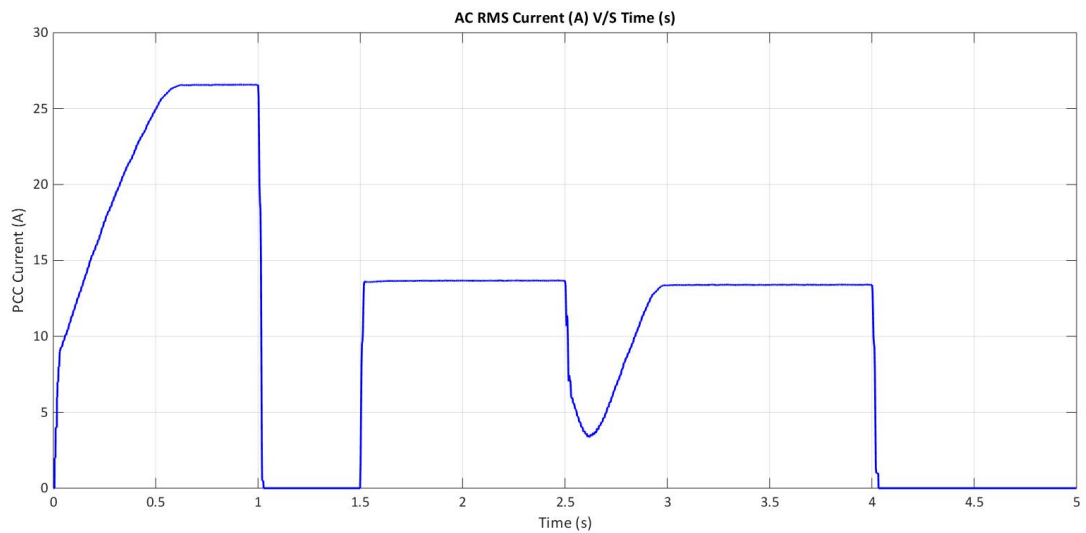


Figure 3.10: AC current (RMS)

The battery is discharging and charging as per given commands on Table 3.1. The RMS value of the PCC current is shown in Fig. 3.10.

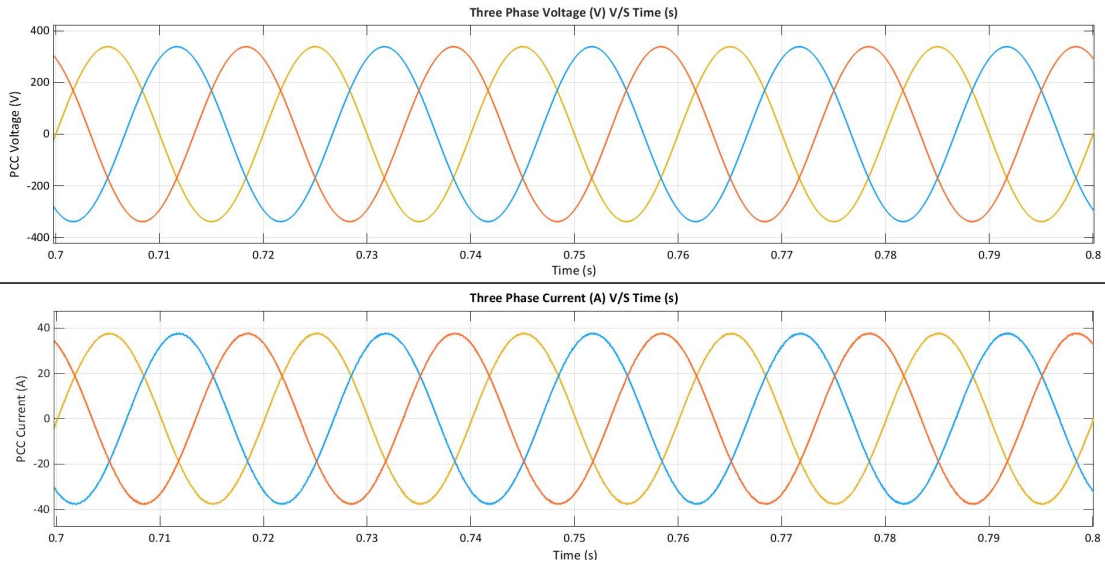


Figure 3.11: PCC voltage and current

The PCC voltage and current waveforms are as shown in Fig. 3.11. It is only for the duration of 1 C battery discharge current. From Fig. 3.11, we can conclude that it is working in the unity power factor mode.

### 3.6 Summary

In this chapter, A bidirectional V2G charger suitable for EV applications has been presented. The discharge schedules of the EV battery obtained from the Peer B energy management formulation in Chapter 2, EV owner can schedule the discharging of battery to gain more economic benefits. The adopted control strategy is simple to implement, but it delivers promising results. From the results obtained, it is clear that the controller's response is good enough in terms of transient and steady-state response. The control strategies of DC-DC and DC-AC bidirectional converter have been explored with practical EV battery data. The chapter has been concluded with the MATLAB simulation results supporting discussions.

## Chapter 4

# Conclusion and Future Work

### 4.1 Conclusion

The thesis addressing the two questions in the area of the energy management in P2P energy trading and grid connected bidirectional converter of an EV, whose answers are mentioned in this section.

The chapter 2 was addressing the some of the draw backs in the existing P2P testbeds. However, ICT framework is neglected in most of the projects. P2P testbed have the hardware layer, controller layer and software layer and it is addressed in the chapter 2. The effectiveness of the proposed model is tested using an experimental setup with three peers having solar PV with a static battery energy storage system (BESS) and EV. Energy management formulation of each peer for cost minimization of electricity from grid also has been presented in the chapter. The integration of the energy meter with the smart agent for the recording of the data is also discussed in the chapter 2. The experimental validation of the discussed algorithm is done by using the historical readings of the solar PV, load. The next day forecasted PV and load values along with the DA and ToU tariff is used as the input of the algorithm. The BESS dispatch from the algorithm results in the cost minimization of electricity. The integration of the P2P testbed with the mobile application and blockchain is also carried out and a case study on the energy trade between two peers is discussed in the chapter. Results reveal that the proposed model provides better economic benefits for the prosumer in comparison to the feed-in tariff (FiT) model.

The power electronic converter design for discharging the EV battery into grid has been discussed in chapter 3. The dq reference frame is used to carry out the control strategies. The EV battery discharging schedules are obtained from the energy management formulation discussed in chapter 2, and smooth power flows should be achieve between grid and EV battery as per schedules obtained from the energy management algorithm. The simulation results shown the desired transient and steady state performance of the EV battery V2G integration.

## 4.2 Scope for Future Work

The testbed at the WTP is fledged with the P2P energy trading setup, and the records of the transactions are stored in the blockchain. However, there is always a possibility of improving the existing systems. Below are some suggestions for future work which can be integrated in the existing testbed.

- Smart plugs and controllers can be integrated in Peers for demand response, and customer can play a significant role by shifting its load as per given signal from DSO to gain the incentives.
- As historical data is updated after every fifteen minutes, rolling time horizon methods could be integrated where forecasting and optimization algorithm and table should run after every fifteen minutes. So, the forecasting and optimization table updated with real time values helps in improvement in solar PV forecasting and load forecasting accuracy.

## **List of Publications**

1. Anandsingh Chauhan, Joice G. Phillip, Ravindra kuhada, and Naran Pindoriya, “Peer to Peer energy trading framework: A Case Study ,” (To be submitted in NPSC 2020)
2. Ravindra kuhada , Anandsingh Chauhan, and Naran Pindoriya, “Real-time simulation of V2G operation for EV battery” (To be submitted in NPSC 2020)
3. Anandsingh Chauhan, Joice G. Phillip, Sachin Suthar, and Naran Pindoriya, “Peer to Peer energy trading using Blockchain,” (Under Preparation)

## Bibliography

- [1] G. R. C. Mouli, P. Bauer, and M. Zeman, "Comparison of system architecture and converter topology for a solar powered electric vehicle charging station," in *2015 9th International Conference on Power Electronics and ECCE Asia (ICPE-ECCE Asia)*, 2015, pp. 1908–1915.
- [2] W. Tushar, B. Chai, C. Yuen, D. B. Smith, K. L. Wood, Z. Yang, and H. V. Poor, "Three-party energy management with distributed energy resources in smart grid," *IEEE Transactions on Industrial Electronics*, vol. 62, no. 4, pp. 2487–2498, 2014.
- [3] T. Morstyn, N. Farrell, S. J. Darby, and M. D. McCulloch, "Using peer-to-peer energy-trading platforms to incentivize prosumers to form federated power plants," *Nature Energy*, vol. 3, no. 2, pp. 94–101, 2018.
- [4] W. Tushar, C. Yuen, H. Mohsenian-Rad, T. Saha, H. V. Poor, and K. L. Wood, "Transforming energy networks via peer-to-peer energy trading: The potential of game-theoretic approaches," *IEEE Signal Processing Magazine*, vol. 35, no. 4, pp. 90–111, 2018.
- [5] T. Sousa, T. Soares, P. Pinson, F. Moret, T. Baroche, and E. Sorin, "Peer-to-peer and community-based markets: A comprehensive review," *Renewable and Sustainable Energy Reviews*, vol. 104, pp. 367–378, 2019.
- [6] E. Mengelkamp, J. Gärttner, K. Rock, S. Kessler, L. Orsini, and C. Weinhardt, "Designing microgrid energy markets: A case study: The brooklyn microgrid," *Applied Energy*, vol. 210, pp. 870–880, 2018.
- [7] H. Beitollahi and G. Deconinck, "Peer-to-peer networks applied to power grid," in *Proceedings of the International conference on Risks and Security of Internet and Systems (CRiSIS)*, vol. 8, 2007.
- [8] C. Zhang, J. Wu, Y. Zhou, M. Cheng, and C. Long, "Peer-to-peer energy trading in a microgrid," *Applied Energy*, vol. 220, pp. 06 2018.
- [9] S. Nguyen, W. Peng, P. Sokolowski, D. Alahakoon, and X. Yu, "Optimizing rooftop photovoltaic distributed generation with battery storage for peer-to-peer energy trading," *Applied Energy*, vol. 228, pp. 2567 – 2580, 2018. [Online]. Available: <http://www.sciencedirect.com/science/article/pii/S0306261918310717>
- [10] C. Long, J. Wu, Y. Zhou, and N. Jenkins, "Peer-to-peer energy sharing through a two-stage aggregated battery control in a community microgrid," *Applied Energy*, vol. 226, pp. 261 – 276, 2018. [Online]. Available: <http://www.sciencedirect.com/science/article/pii/S0306261918308146>



- [11] Thakur, Subhasis, Breslin, and J. G., “Peer to Peer Energy Trade Among Microgrids Using Blockchain Based Distributed Coalition Formation Method,” *Technology and Economics of Smart Grids and Sustainable Energy*, vol. 3(1), p. 5, 2018.
- [12] A. Paudel, K. Chaudhari, C. Long, and H. B. Gooi, “Peer-to-peer energy trading in a prosumer-based community microgrid: A game-theoretic model,” *IEEE Transactions on Industrial Electronics*, vol. 66, no. 8, pp. 6087–6097, 2019.
- [13] W. Tushar, T. K. Saha, C. Yuen, T. Morstyn, H. V. Poor, R. Bean *et al.*, “Grid influenced peer-to-peer energy trading,” *IEEE Transactions on Smart Grid*, vol. 11, no. 2, pp. 1407–1418, 2019.
- [14] H. Liu, J. Li, S. Ge, X. He, F. Li, and C. Gu, “Distributed day-ahead peer-to-peer trading for multi-microgrid systems in active distribution networks,” *IEEE Access*, vol. 8, pp. 66 961–66 976, 2020.
- [15] J. Guerrero, A. C. Chapman, and G. Verbič, “Decentralized p2p energy trading under network constraints in a low-voltage network,” *IEEE Transactions on Smart Grid*, vol. 10, no. 5, pp. 5163–5173, 2018.
- [16] A. Lüth, J. M. Zepter, P. C. del Granado], and R. Egging, “Local electricity market designs for peer-to-peer trading: The role of battery flexibility,” *Applied Energy*, vol. 229, pp. 1233 – 1243, 2018. [Online]. Available: <http://www.sciencedirect.com/science/article/pii/S0306261918311590>
- [17] E. Sorin, L. Bobo, and P. Pinson, “Consensus-based approach to peer-to-peer electricity markets with product differentiation,” *IEEE Transactions on Power Systems*, vol. 34, no. 2, pp. 994–1004, 2018.
- [18] T. Chen and W. Su, “Indirect customer-to-customer energy trading with reinforcement learning,” *IEEE Transactions on Smart Grid*, vol. 10, no. 4, pp. 4338–4348, 2018.
- [19] R. Alvaro-Hermana, J. Fraile-Ardanuy, P. J. Zufiria, L. Knapen, and D. Janssens, “Peer to peer energy trading with electric vehicles,” *IEEE Intelligent Transportation Systems Magazine*, vol. 8, no. 3, pp. 33–44, 2016.
- [20] T. Basso, *IEEE 1547 and 2030 Standards for Distributed Energy Resources Interconnection and Interoperability with the Electricity Grid*.
- [21] SAE J2894, “Power Quality Requirements for Plug-In Electric Vehicle Chargers,” 2011., SAE, 2019. [Online]. Available: [https://www.sae.org/standards/content/j2894/1\\_201901/](https://www.sae.org/standards/content/j2894/1_201901/)
- [22] Agilent AN 1273 Compliance Testing to the IEC 1000-3-2 (EN 61000-3-2) and IEC 1000-3-3 (EN 61000-3-3) Standards. [Online]. Available: <http://literature.cdn.keysight.com/litweb/pdf/5964-1917E.pdf>
- [23] M. Yilmaz and P. T. Krein, “Review of battery charger topologies, charging power levels, and infrastructure for plug-in electric and hybrid vehicles,” *IEEE transactions on Power Electronics*, vol. 28, no. 5, pp. 2151–2169, 2012.

- [24] J. Kang, R. Yu, X. Huang, S. Maharjan, Y. Zhang, and E. Hossain, “Enabling localized peer-to-peer electricity trading among plug-in hybrid electric vehicles using consortium blockchains,” *IEEE Transactions on Industrial Informatics*, vol. 13, no. 6, pp. 3154–3164, 2017.
- [25] “Develop and demonstrate a block-chain based peer to peer energy sharing and trading platform that enables consumers to manage their home or industrial energy needs.” [Online]. Available: <https://www2.iima.ac.in/p2penergy/index.php>
- [26] S. Suthar, N. Kumar, and N. M. Pindoriya, “Cost-effective energy management of grid-connected pv and bess: A case study,” in *2019 IEEE Innovative Smart Grid Technologies - Asia (ISGT Asia)*, 2019, pp. 4122–4127.
- [27] *Internal documentation for MinimalModbus*. [Online]. Available: <https://minimalmodbus.readthedocs.io/en/stable/internalminimalmodbus.html>
- [28] B. Kramer, S. Chakraborty, and B. Kroposki, “A review of plug-in vehicles and vehicle-to-grid capability,” in *2008 34th Annual Conference of IEEE Industrial Electronics*, 2008, pp. 2278–2283.
- [29] S. Habib, M. Kamran, and U. Rashid, “Impact analysis of vehicle-to-grid technology and charging strategies of electric vehicles on distribution networks—a review,” *Journal of Power Sources*, vol. 277, pp. 205–214, 2015.
- [30] M. C. Kisacikoglu, B. Ozpineci, and L. M. Tolbert, “Examination of a phev bidirectional charger system for v2g reactive power compensation,” in *2010 Twenty-Fifth Annual IEEE Applied Power Electronics Conference and Exposition (APEC)*, 2010, pp. 458–465.
- [31] Y.-M. Wi, J.-U. Lee, and S.-K. Joo, “Smart electric vehicle charging for smart home/building with a photovoltaic system,” *Consumer Electronics, IEEE Transactions on*, vol. 59, pp. 323–328, 05 2013.
- [32] M. A. Khan, I. Husain, and Y. Sozer, “Integrated electric motor drive and power electronics for bidirectional power flow between the electric vehicle and dc or ac grid,” *IEEE Transactions on Power Electronics*, vol. 28, no. 12, pp. 5774–5783, 2013.
- [33] A. Sharma and S. Sharma, “Review of power electronics in vehicle-to-grid systems,” *Journal of Energy Storage*, vol. 21, pp. 337 – 361, 2019. [Online]. Available: <http://www.sciencedirect.com/science/article/pii/S2352152X1830481X>
- [34] W. Kempton, V. Udo, K. Huber, K. Komara, S. Letendre, S. Baker, D. Brunner, and N. Pearre, “A test of vehicle-to-grid (v2g) for energy storage and frequency regulation in the pjm system,” *Results from an Industry-University Research Partnership*, vol. 32, 2008.
- [35] S. Gao, K. Chau, C. Liu, D. Wu, and C. C. Chan, “Integrated energy management of plug-in electric vehicles in power grid with renewables,” *IEEE Transactions on Vehicular Technology*, vol. 63, no. 7, pp. 3019–3027, 2014.

- [36] C. Liu, K. T. Chau, D. Wu, and S. Gao, “Opportunities and challenges of vehicle-to-home, vehicle-to-vehicle, and vehicle-to-grid technologies,” *Proceedings of the IEEE*, vol. 101, no. 11, pp. 2409–2427, 2013.
- [37] M. Yilmaz and P. T. Krein, “Review of the impact of vehicle-to-grid technologies on distribution systems and utility interfaces,” *IEEE Transactions on Power Electronics*, vol. 28, no. 12, pp. 5673–5689, 2013.
- [38] E. Apostolaki-Iosifidou, P. Codani, and W. Kempton, “Measurement of power loss during electric vehicle charging and discharging,” *Energy*, vol. 127, pp. 730 – 742, 2017. [Online]. Available: <http://www.sciencedirect.com/science/article/pii/S0360544217303730>
- [39] G. R. C. Mouli, J. Kaptein, P. Bauer, and M. Zeman, “Implementation of dynamic charging and v2g using chademo and ccs/combo dc charging standard,” in *2016 IEEE Transportation Electrification Conference and Expo (ITEC)*, 2016, pp. 1–6.
- [40] C. Guille and G. Gross, “A conceptual framework for the vehicle-to-grid (v2g) implementation,” *Energy Policy*, vol. 37, no. 11, pp. 4379 – 4390, 2009. [Online]. Available: <http://www.sciencedirect.com/science/article/pii/S0301421509003978>